

**YILDIRIM BEYAZIT UNIVERSITY  
GRADUATE SCHOOL OF NATURAL AND APPLIED  
SCIENCES**

**INVESTIGATION OF THE EFFECTS OF  
HOLDING TIMES AT CRYOGENIC  
TEMPERATURES ON RESIDUAL STRESS  
DISTRIBUTION OF AISI D2 TOOL STEEL**

**By  
Eylül DEMİR**

**January, 2014  
ANKARA**

**INVESTIGATION OF THE EFFECTS OF  
HOLDING TIMES AT CRYOGENIC  
TEMPERATURES ON RESIDUAL STRESS  
DISTRIBUTION OF AISI D2 TOOL STEEL**

**A Thesis Submitted to the  
Graduate School of Natural and Applied Sciences of Yıldırım Beyazıt  
University  
In Partial Fulfillment of the Requirements for the Degree of Master of Science  
in Mechanical Engineering, Department of Mechanical Engineering**

**by  
Eylül DEMİR**

**January, 2014**

**ANKARA**

## M.Sc THESIS EXAMINATION RESULT FORM

We have read the thesis entitled “**THESIS TITLE**” completed by **STUDENT NAME** under supervision of **TITLE AND NAME OF THE SUPERVISOR** and we certify that in our opinion it is fully adequate, in scope and in quality, as a thesis for the degree of Master of Science.

.....  
Assist. Prof. Dr. İhsan TOKTAŞ

\_\_\_\_\_  
Supervisor

.....  
Prof. Dr. A. Tamer ÖZDEMİR

\_\_\_\_\_  
(Jury Member)

.....  
Assoc. Prof. Dr. Adem ÇİÇEK

\_\_\_\_\_  
(Jury Member)

.....  
Prof.Dr. Fatih V. ÇELEBİ

Director

Graduate School of Natural and Applied Sciences

## ACKNOWLEDGEMENTS

I would like to thank all those people who made this thesis possible and provided an important experience for me.

First of all, I would like to express the deepest appreciation to my advisor Assist. Prof. Dr. İhsan TOKTAŞ for his guidance, understanding, patience. He always shared his knowledge and experience with me at every steps of my thesis.

Besides my advisor, I am deeply grateful to Assoc. Prof. Dr. Adem ÇİÇEK for his guidance during all stage of my thesis.

I want to thank to Academicians of Technology Faculty of Gazi University. Prof. Dr. Tamer ÖZDEMİR and Assoc. Prof. Dr. Çetin KARATAŞ gave insightful comments and suggestions about my results and discussions.

Finally, my heartfelt appreciation goes to **my dear father** whose love and longing I keep in my heart during all of my life.

## Abstract

AISI D2 is cold tool work steel and is used widely due to the advantages such as its wear resistance, compressive strength and toughness.

When the literature is reviewed, it is observed that researches associated with the effect of cryogenic treatment on residual stress are rather poor. Residual stress is very important since this affects some properties such as fatigue life, wear resistance, crack propagation and stress corrosion which determine the service life of materials.

In this study, effect of the holding time at cryogenic temperatures on residual stress of AISI D2 cold work tool steel is investigated. Results shows that tensile residual stress on surface of AISI D2 steel decreases with cryogenic treatment and subsequently turns into compressive residual stress on subsurface. While residual stress value on surface of the specimen for holding time ( $t_{CT}$ ) of 24 h is 242.3 MPa in axial direction and 172.5 MPa in tangential direction, and in specimen conventionally treated is 321.5 MPa in axial direction and 316.8 MPa in tangential direction. There is no significant difference between hardness values, but carbide precipitation increases in specimen cryotreated for  $t_{CT}=24$  h. Apart from this, surface roughness improves for cryogenic treatment. In comparison to conventional heat treatment and cryogenic treatment at various holding times,  $t_{CT}=24$  h has better results regarding residual stress, carbide precipitation, and surface roughness.

Keywords: AISI D2 steel, cryogenic treatment, residual stress, carbide precipitation, surface roughness.

## ÖZ

Bu çalışmada, farklı bekletme sürelerindeki kriyojenik işlemin AISI D2 çeliğinin kalıntı gerilmelerine, sertliğine ve mikro yapısına etkisi araştırılmıştır. Aynı zamanda, taşlanan numunelerin yüzey pürüzlülüğündeki değişim incelenmiştir. Klasik ısıl işlem ve diğer bekletme süreleri ile karşılaştırıldığında, 24 saat bekletme süresi, kalıntı gerilme, karbür dağılımı ve yüzey pürüzlülüğü açısından daha iyi sonuçlar vermiştir.

Anahtar kelimeler: AISI D2 çeliği, kriyojenik işlem, kalıntı gerilme, karbür dağılımı, yüzey pürüzlülüğü

## CONTENTS

THESIS EXAMINATION RESULT FORM .....	ii
ACKNOWLEDGEMENTS .....	iii
ABSTRACT .....	iv
ÖZ .....	v
CONTENTS .....	vi
LIST OF TABLES .....	vii
LIST OF FIGURES .....	viii
<b>1. INTRODUCTION .....</b>	<b>1</b>
<b>2. DESCRIPTIONS .....</b>	<b>14</b>
2.1 Cryogenic Treatment .....	14
2.2 Residual Stress .....	15
2.2.1 The effect of Residual Stress on Working Performance .....	19
2.2.2 Measurement Methods for Residual Stresses .....	20
2.2.2.1 Non-destructive Methods of Residual Stress Measurement .....	22
2.2.2.1.1 X-Ray Diffraction Method (XRD) .....	22
2.2.2.1.2 Neutron Diffraction Method (XRD) .....	24
2.2.2.1.3 Ultrasonic Method .....	25
2.2.2.1.4 Magnetic Barkhausen Noise Method .....	25
2.2.2.1.5 Raman Spectrum Method .....	27
2.2.2.2 Destructive Methods of Residual Stress Measurement .....	27
2.2.2.2.1 Layer Removal Method .....	27
2.2.2.2.2 Hole Drilling Method .....	28
2.2.2.2.2.a Hole Drilling Method via Strain Gages .....	28
2.2.2.2.2.b Hole Drilling Method with ESPI technique .....	32
2.2.2.2.3 Ring Core Method .....	35
2.2.2.2.4 Sectioning Method .....	36
2.2.2.2.5 Slitting or Crack Compliance Method .....	37

2.2.2.2.6 Contour Method .....	38
2.2.3 Comparison of Residual Stress Measurement Methods .....	39
<b>3. EXPERIMENTAL PROCEDURES .....</b>	<b>40</b>
3.1 Materials .....	40
3.2 Measurement of Residual Stress .....	46
3.3 Microstructure Examination.....	50
3.4 Hardness Measurement.....	51
3.5 Grinding the Specimens and Measurement of Surface Roughness.....	53
<b>4. RESULTS and DISSCUSSIONS .....</b>	<b>55</b>
4.1 Residual Stress Values.....	55
4.2 Microstructural Characteristics .....	58
4.3 Retained Austenite.....	64
4.4 Hardness Values .....	65
4.5 Surface Roughness Values.....	66
4.6 Correlations of Microstructure and Hardness .....	67
4.7 Correlations of Microstructure and Residual Stress .....	67
4.8 Correlations of Microstructure, Hardness Residual Stress and Surface Roughness .....	68
4.9 Conclusions .....	68
4.10 Recommendations .....	69
<b>REFERENCES .....</b>	<b>70</b>
<b>APPENDIX .....</b>	<b>80</b>
Appendix 2.1. Analysis formulas of hole drilling method .....	81

## LIST OF TABLES

2.1 Comparison of residual stress measument methods .....	39
3.1 Chemical composition of AISI D2 steel .....	40
3.2 Physical properties of AISI D2 steel .....	40



3.3 Treatments applied to specimens .....	41
3.4 Analysis parameters for XRD .....	48
3.5 Effects of sub-zero treatments on hardness of steels .....	51

## LIST OF FIGURES

2.1 Stress components in a material .....	16
2.2 Different kinds of residual stress .....	17
2.3 Macro stresses in a layer (continuous lines) and micro stresses (dashed lines) .	18
2.4 Superposition of residual stress and applied stress .....	19
2.5 Determination of residual stress using X-ray diffraction method .....	23
2.6 Planes carrying out Bragg's Law .....	24
2.7 Domains and magnetic dipoles in a ferromagnetic material .....	26
2.8 Orientation of domains in a scattered situation (left) orientation of domains according to magnetic field (right) .....	26
2.9 Layer removal from a rectangular component (above) Layer removal from a cylindrical component .....	28
2.10 Three dimensional view of hole drilling .....	29
2.11 Schematic view of strain gages .....	30
2.12 Variation of tangential and axial strains relaxation moving away center of the hole .....	31
2.13 Determination of displacement map .....	33
2.14 Schematic view of the ESPI system .....	33
2.15 Fringe patterns .....	34
2.16 Hole drilling method (left) and ring core method (right).....	35
2.17 Schematic view of sectioning method .....	36
2.18 Schematic view of slitting or crack compliance method .....	37
2.19 Schematic view of contour method .....	38
3.1 Dimensions of specimens .....	41
3.2 Classification of samples before treatments .....	42
3.3 Conventional heat treatment (austenization+tempering) .....	43

3.4 Cryogenic cooling furnace (above) and temperature-pressure indicator (below)	44
3.5 Austenization+cryogenic treatment+tempering	45
3.6 Cryogenic treatment at various holding times	45
3.7 Selection of tempering temperature	46
3.8 Residual stress measurement with XRD	47
3.9 Hole drilling equipment	49
3.10 Microstructure examinations	50
3.11 Macro hardness tester	52
3.12 Average surface roughness value, $R_a$	53
3.13 Calibration of tester	54
3.14 Measurement of surface roughness	54
4.1 Residual stress in axial direction	55
4.2 Surface residual stress in axial direction	56
4.3 Residual stress in tangential direction	57
4.4 Surface residual stress in tangential direction	57
4.5 Microstructure of specimens (X500 magnification)	61
4.6 Microstructure of specimens (X1000 magnification)	63
4.7 Retained austenite	64
4.8 Macro hardness values of AISI D2 steel	65
4.9 Average surface roughness ( $R_a$ ) of AISI D2 steel	66

## CHAPTER 1

### 1. Introduction

Reducing the production cost and the growing demand for higher productivity requires researches oriented to enhance the tool life and performance. Current studies are carried out for developing new materials beside the already existing ones by changing the production methods for engineering particles with longer service life (Das et al., 2009a). An increase in the service life of the tools, not only decreases the cost but also the downtime, thus it paves the way for a growth in productivity (Das and Ray, 2012a).

AISI D2 steel which is a cold work tool steel is used in this study. Because of its cost and features, AISI D2 has been widely used in press forming dies (Gauthier, 1995). The reasons for choosing this type of a steel can be listed as follows:

- (i) AISI D2 steel is one of the most widely used cold work tool steel especially in trimming knives, slitting cutters and in punching, drawing, coining and blanking dies (Pan et al., 1998; Sen et al., 2001).
- (ii) AISI D2 steel is one of the most widely used materials of tool/die steels the wear resistance of which is searched in subzero treatment (Das et al., 2008).
- (iii) The improvement degree for wear resistance of tool/die steels subjected to cryogenic treatment is quite high for AISI D2 steel (Das et al., 2009b).

Research works performed in the last two decades have proved that the service life of tool/die steels can be immensely enhanced by applying cryogenic treatment to engineering materials after conventional hardening and tempering (Das et al., 2009c). Sub-zero treatments are generally divided into two as cold treatment (193-223 K) and cryogenic treatment (77-193 K). Cryogenic treatment is further classified into two as shallow cryogenic treatment (113-193 K) and deep cryogenic treatment (77-113 K) (Das et al., 2009). Temperature values of deep cryogenic treatment between 77-148 K are accepted to be among the values and these are also presented in the

researches (Collins, 1996; Collins and Dormer, 1997; Moore and Collins, 1993; Yen, 1997).

The material in cryogenic treatment is cooled in sub-zero temperatures and is held under this temperature for a certain period of time then the temperature is turned back to room temperature. The aim of cryogenic treatment is to get the desired features from the material by making permanent changes in the micro structure of the material with minimum negative effect (Thornton et al., 2011).

In tool/die steels containing high carbon and alloy elements, martensite finish temperature falls under the surrounding temperature. Conventional hardening treatment results in retained austenite in undesired quantities. As retained austenite is a soft phase, it negatively affects wear resistance and toughness of materials (Roberts et al., 1998; Thelning, 1984). For this reason, the main purpose of heat treatment for tool/die steels is to decrease the retained austenite to a minimum degree or to eliminate it completely (Das et al., 2009a, 2009c, 2009d, 2009e, 2010a, 2010b; Das et al., 2007; Das and Ray, 2012a, 2012b; Das et al., 2009; Das et al., 2010).

On the other hand, the martensite transformation of austenite, causes dimensional changes and deformity in particles (Roberts et al., 1998; Thelning, 1984). These deformations seen in crystal structure are due to increase in volume by 4% (Popandopulo and Zhukova, 1980). In the studies carried out so far, it is seen that the quantity of retained austenite in AISI D2 steel is decreased by cryogenic treatment (Das et al., 2009a, 2009c, 2009d, 2009e, 2010b; Das et al., 2007; Das and Ray, 2012a, 2012b; Das et al., 2009; Das et al., 2010; Oppenkowski, et al., 2010) and nearly all is removed by deep cryogenic treatment (Das et. al, 2009d, 2010a; Das and Ray, 2012b).

The effect of sub-zero treatments and tempering numbers on retained austenite, applied in various degrees and holding periods for AISI D2 steel in -90 °C, -120 °C and in -150 °C for 25 minutes and in -150 °C for 24 hours is analysed. The amount of retained austenite is decreased to 1% after single tempering treatments applied as a

continuation to sub-zero treatments. No change in the amount of retained austenite was seen in tempering treatments carried out more than once (Surberg et al., 2009).

Besides it is seen that in cryogenic treatment, the amount of secondary carbides in microstructure of AISI D2 steel increases and a more dense distribution happens (Das et al., 2009a, 2009c, 2010a, 2009d, 2009e, 2010b; Das et al., 2007; Das and Ray, 2012a, 2012b; Das et al., 2009; Das et al., 2010). In deep cryogenic treatment, in comparison with conventional heat treatment, cold treatment and shallow cryogenic treatment, a denser and a more homogeneous secondary carbide distribution is observed (Das and Ray, 2012a; Das et al., 2010b; Das et al., 2009).

Sub-zero treatments does not only affect the amount of retained austenite in steels but it also affects the decomposition of martensite, changing the precipitation behaviour of secondary carbides (carbides smaller than 5  $\mu\text{m}$ ) during tempering. Among sub-zero treatments, the effect on carbide distribution increases with cold treatment, shallow cryogenic treatment and deep cryogenic treatment, respectively. High density crystal defects like dislocations occurs in martensite during sub-zero treatments. Because of the transformation of austenite to martensite and various heat decrements of phases, high internal stresses happen. An increase in these effects is observed, because the heat of sub-zero treatment decreases due to the transformation of austenite to martensite rather than the increase in heat decrements (Das et al., 2009a, 2010a; Huang et al., 2003).

In low temperature, martensite is more saturated and this respectively increases lattice deformations and thermodynamic instability which causes the carbon atoms to split into fault of clusters. These clusters becomes cores to form carbides when there is enough heating or during tempering. The number of atomic clusters increases when the temperature of sub-zero treatment decreases and when the holding period in the lowest temperature lengthens. Thus, decomposition of martensite will be faster with cold treatment, shallow cryogenic treatment and deep cryogenic treatment, respectively and as a result more carbide precipitation will be gathered again with the same order (Das et al., 2009a; Huang et al., 2003; Das et al., 2010a). In steels with

cryogenic treatment, crystal defects in high densities are observed in experiments (Yun, 1998; Rhyim, 2006), therefore, this suggestion is supported by the necessity of long holding periods to benefit from cryogenic treatment (Mohan Lal et al., 2001; Collins, 1996; Collins and Dormer, 1997; Das et al., 2009e; Surberg et al., 2008).

Mohan Lal et al. (2001) and Yun et al. (1998) showed that in deep cryogenic treatment, retained austenite turned into martensite and fine carbides precipitated while the martensite was broken into pieces. Huang et al. (2003), indicated that cryogenic treatment did not only enable carbide formation but it also increased the density and volumetric proportion of carbides in martensite matrix of M2 steel. Besides Huang et al. (2003) proved that cryogenic treatment generated a more homogenous dissipation. Paulin (1993) analysed the effects of fine precipitated carbide particles on the properties of tool steel. It was found indicated that fine carbide precipitation increased wear resistance and decreased the internal stress in martensites and thus the sensitivity of micro cracks decreased at the same time.

According to Rhyim et al. (2006), cryogenic treatment increased the necessary power for carbide nucleation and enabled more and finer carbide precipitation and as a result toughness increased which in turn increased wear resistance. Collins and Dormer (1997) reported that when the holding period of cryogenic treatment applied to AISI D2 steel was increased, the density of fine carbides would also increase. Yun et al. (1998) suggested that longer holding periods were required for fine carbide precipitation. Different from the transformation of retained austenite to martensite, the formation of fine carbide is a situation which depends on time.

Meng et al. (1994), analysed the structure of AISI D2 steel which went through conventional heat treatment, cold treatment and deep cryogenic treatment. In specimens on which deep cryogenic treatment was applied,  $\eta$ -carbide (eta carbide) was seen in specimens, precipitated in the shape of very thin bar. However no carbide precipitation was detected in specimen to which conventional heat treatment and cold treatment was applied. In both of these two treatments, carbon-rich and carbon-poor regions were seen because of spinodal decomposition of martensite.

Nevertheless,  $\eta$ -carbides, as in tempering AISI D2 steel for 30 minutes in 180°C (453 K) (Meng et al., 1994) are formed in the initial tempering of hardened steel (Cheng et al., 1988; Cheng et al., 1991; Taylor et al., 1989). These researches (Unterweiser et al., 1987) applied tempering temperatures below the temperatures suggested for AISI D2 steel (between 205-540 °C (478-813 K)). In the researches, not any eta carbides was seen in the same steel to which sub-zero heat treatments was applied (Das et al., 2007; Das et al., 2009; Collins and Dormer, 1997; Rhyim et al., 2006) and not applied (Tiziani and Molinari, 1988; Fukaura et al., 2004) for higher temperatures and longer tempering periods than those of Meng et al. (1994). As eta carbides are instable, they transform into cementite or to alloy carbides which are more stable in tempering treatments (Reed-Hill and Abbaschian, 1992; Das et al., 2009; Cheng et al., 1988; Taylor et al., 1989; Rhyim et al., 2006).

There are a limited number of studies with contradictory results on the hardness of tool/die steels depending on the holding period in cryogenic treatment. Kamody (1993), claimed that the holding period did not affect macro hardness, however Moore and Collins (1993) asserted that hardness was affected in accordance with the chemical structure of the steel used. Also as the holding period is prolonged, hardness of H13 steel increases but it does not change in Vanadis-4 and D2 steels. In contrast, Collins and Dormer (1997) proved that together with the holding period hardness of AISI D2 steel increased and the degree of recovery and the type of variance were in relation with austenitizing temperature. Yun et al. (1998) applied cryogenic treatment to AISI T1 and M2 steels for 24 and 48 hours and in 48 hours holding period he recorded 0.2 HRC variance in hardness.

Molinari et al. (2001), reported that deep cryogenic treatment, in comparison with conventional heat treatment, increased the hardness of AISI M2 and H13 steels by 5.8% and 3% respectively. Baldissera and Delprete (2008) indicated that the hardness of steel 18NiCrMo5 increased by 4.1% increment by means of deep cryogenic treatment in comparison with conventional heat treatment. The 3,1% and 1,6% increment in hardness of 4340 steel occurred in accordance with tempering temperature (Zhirafar et al., 2007). Nevertheless, in sub-zero treatments, there are

different ideas about the changes of hardness in relation with heat. Akhbarizadeh et al. (2009) reported that the improvement in the hardness of D3 steel was more in deep cryogenic treatment in comparison with cold treatment and the same result was also gathered in En 31 steel by Harish et al. (2009). On the contrary, Bensely et al. (2005) pointed that not any improvement was seen in the hardness of En 353 steel in cold and deep cryogenic treatment in comparison with conventional heat treatment. Collins and Dormer (1997) reported that in sub-zero treatments when the temperature decreased to  $-80\text{ }^{\circ}\text{C}$  ( $193\text{ K}$ ) the hardness increased but no changes in hardness appeared in temperatures lower than this one. On the contrary, Moore and Collins (1993) showed that hardness in shallow cryogenic treatment applied in  $-140^{\circ}\text{C}$  ( $133\text{ K}$ ) is higher than the hardness in deep cryogenic treatment applied in  $-196^{\circ}\text{C}$  ( $77\text{ K}$ ) and in cold treatment applied in  $-80^{\circ}\text{C}$  ( $223\text{ K}$ ).

The opponent reports, about the variance in hardness of tool/die steels under different sub-zero treatments, is thought to be formed by the changes in parameters of sub-zero treatments together with the parameters of tempering and hardness treatments. The effect of parameters of sub-zero treatments such as the holding period at the lowest temperature has been the subject in some researches (Das et al., 2009c, 2009e). Furthermore, it is known that the hardness of tool/die steels depends on the amount, dimension and dispersion of primary and secondary carbides and on retained austenite and tempered martensite phases (Roberts et al., 1998; Thelning, 1984; Red-Hill, 1992). These properties are affected by (i) austenitizing temperature and duration (ii) quenching (iii) tempering temperature and duration and besides the number of tempering (Das et al., 2010a).

The number of studies, about the already mentioned parameters on the microstructure components and mechanical properties of steels, is quite few. Collins and Dormer (1997) searched for the effect of austenitizing temperature on the hardness and microstructure of AISI D2 steel to which conventional heat treatment and different sub-zero treatments were applied. As austenizing temperature increase, the hardness difference between conventional heat treatment and deep cryogenic treatment increased. This increment in austenitizing temperature also caused an



increase in retained austenite amount. Surberg et al. (2008) also obtained the same results in his study. The concurrent increment in austenitizing temperature of tool/die steels with the increase in the amount of retained austenite is a familiar situation (Roberts et al., 1998; Thelning, 1984; Reed-Hill, 1992; Bowes, 1974; Das et al., 2007; Carlson, 1990). High austenitizing temperatures cause a further dispersion of primary carbides, and increase the alloy elements and the level of carbon in austenite phase. Thus it increases the stability of austenite or lowers the martensite finish temperature. Therefore the degree of martensite transformation of austenite with hardening treatment would be lower and as a consequence the amount of retained austenite in hardened steels would be higher.

Surberg et al. (2008) also analysed the effects of sub-zero treatment temperature and the number of tempering on the amount of retained austenite in AISI D2 steel. For higher austenizing temperatures, as a consequence of hardening with sub-zero treatments (rather than conventional heat treatment) applied by cooling down to -120 °C (153 K), although a significant decrease in the amount of retained austenite is seen, it has not been effective on transforming the entire austenite to martensite. To transform the entire retained austenite, double-tempering is necessary in conventional heat treatment, whereas single-tempering is required in specimens with sub-zero treatments (Surberg et al., 2008).

Rhyim et al. (2006) analysed the effect of tempering temperatures to hardness and microstructure of AISI D2 steel to which conventional heat treatment, cold treatment and deep cryogenic treatment was applied. When hardened specimens are tempered in high temperatures, he mentioned that both sub-zero treatments did not have any different effect on retained austenite than conventional heat treatment. The increment in tempering temperature decreased the hardness of AISI D2 steel which is hardened by various treatments, but the change in hardness was different both for deep cryogenic treatment and for conventional heat treatment. For this reason, optimal parameters for various types of sub-zero treatments and conventional heat treatment are different.

Das et al. (2007) indicated that cryogenic treatment in comparison to conventional heat treatment provide 5% increase in hardness of AISI D2 steel. But there was no significant difference between holding times for 36 h and 84 h. Deep cryogenic treatment in comparison to other sub-zero treatments (shallow cryogenic treatment and cold treatment) ensure optimal improvement in hardness. Increase in hardness was %8.1 according to conventional heat treatment (Das et al., 2010a). Bensely (2010) suggested that variation in harness of specimens cryotreated was negligible.

The effect of sub-zero treatments in wear resistance of tool/die steels has been studied on a large scale recently and it is particularly seen that a significant increase takes place with deep cryogenic treatment (Das et al., 2010b; Das et al., 2007). Wear resistance has increased because of cryogenic treatment which decreased the amount of retained austenite and improved the secondary carbide precipitation (Das and Ray, 2012a, 2012b; Das et al., 2009c, 2009d, 2010b). Different holding times (0, 12, 36, 63, 84 and 132) in deep cryogenic treatment (77K) applied to AISI D2 steel is done to find the best holding time for wear resistance. The improvement in wear resistance is associated with the density and size of carbide particles (Das and Ray, 2012a; Das et al., 2009c) and with toughness of the material. It is found that optimum holding time is 36 hours (Das et al., 2009c, 2010b; Oppenkowski et al., 2010).

Furthermore the effect of cryogenic treatment temperature on wear resistance of AISI D2 steel was studied and it is reported that lower temperatures are better in improving the wear resistance (Das et al., 2009d, 2010b; Das et al., 2009). The degree of improvement in wear resistance in ascending order is as follows: conventional heat treatment, cold treatment, shallow cryogenic treatment and deep cryogenic treatment (Das et al., 2009d, 2010b). A better improvement is observed in wear resistance when the amount of austenite is minimum and the amount of secondary carbide is more and denser in deep cryogenic treatment (Das et al., 2009d, 2010b; Das et al., 2009).

Tool life and wear resistance of D3 and M2 steels were analyzed by applying cryogenic treatment (6 and 24 hours). It is observed that the holding period is a much

more effective parameter than cooling down the temperature in cryogenic treatment (Mohan Lal et al., 2001). It is seen that the wear resistance of AISI D2 steel has increased in 77 K as with the holding time. In addition, an increase in the holding time also caused an increase in the precipitation of fine carbides (Collins and Dormer, 1997). Again, in a study in which the effect of holding time was analysed, it is reported that intensive carbide dissolution is a structure formation of which is based on time (Yun et al., 1998).

Taguchi method is used in determining the main factors of cryogenic treatment affecting the wear resistance and mechanical properties of powder metallurgically produced cold work tool steel AISI D2. Austenitizing temperature, cooling rate, holding time (0, 1, 5, 24, 36, 48, 72 hours), heating rate and tempering temperature are the factors studied. It is seen that austenitizing and tempering temperature are the most distinctive parameters affecting the properties of tool steel (Oppenkowski et al., 2010).

Fracture toughness is an important property of tool/die steels. Because the wear resistance of these types of steel is not only based on toughness but also it is based on fracture toughness. In addition, some of the most common faults in tool/die steels like chipping, galling and cracking, can be controlled with fracture toughness (Das et al., 2010). When the various sub-zero treatments applied to AISI D2 steel (cold treatment, shallow cryogenic treatment, deep cryogenic treatment) are compared with conventional heat treatment, it is seen that the fracture toughness increases with deep cryogenic treatment (Das and Ray, 2012a; Das et al., 2010). Besides, this increment in fracture toughness is attributed to the increment in ductility of the matrix, together with the refined carbide distribution (Das and Ray, 2012a; Das et al., 2010) and decrease in the amount of retained austenite (Das and Ray, 2012a). In another related study, a significant difference was not observed in the fracture toughness of both cryotreated and noncryotreated AISI D2 specimens (Oppenkowski et al., 2010).

It is known that failures in service conditions originate from surfaces by means of mechanisms such as wear resistance, fatigue crack, corrosion, and erosion. Therefore, determination of suitability of surfaces has a great importance. Surfaces both obtained with machining and problems caused by working with raise the importance of this subject (Akdoğan, 2005).

Surface roughness for forming members such as dies working in serious conditions is a property which must be taken into account. It is known that surface roughness of a forming member affects the material (Akdoğan, 2005).

Stress values can be cause to crack even above tensile and yield strength. The reason is fatigue. At the head of the factors effecting fatigue comes surface properties. Smoother surface provides a higher fatigue strength (Akdoğan, 2005).

Surface roughness is an important case that effects the factors such as friction, lubrication, heat and electrical conduction in the service conditions. (Choudhury and Bajpai, 2005; Özay et al., 2011).

In a research, it was examined the effects of conventional heat treatment, shallow cryogenic treatment and deep cryogenic treatment applied to En 353 steel on grinding. It was also seen in the micrographs taken by optical microscope that untempered specimens of shallow cryogenic treatment and deep cryogenic treatment have surface cracks which cause miserable effects in terms of component life. Formation of surface cracks on surfaces of untempered specimens was explained with that transformation of retained austenite to martensite render the structure brittle in the components exposed to low temperature. Specimen tempered and conventionally treated is more brittle than specimens tempered and sub-zero treated because of the less precipitation of carbides (Bensely et al., 2008).

Recently, material scientists and engineers have made an effort to increase the fatigue life and impact properties of metals by creating a compressive residual stress on the surface of the metals. Residual stress is the stress observed within the material

when other stress causing factors like heat change and external forces are eliminated. Residual stress occurs due to irregular plastic deformation during cold treatment, shot peening, surface hammering, welding, grinding, phase transformations and high heat transformations. Taking the residual stress in steels into account is quite significant for part design and this provides an improvement not only in fatigue resistance but also in dimensional stability of the materials (Senthilkumar et al., 2011).

In a study, the effect of shallow cryogenic treatment (-80 °C, 5 hours) and deep cryogenic treatment (-196 °C, 24 hours), on residual stress, applied to 4140 steel, is examined. As the cryogenic treatment temperature decreases more austenite is transformed to martensite and the most compressive residual stress is seen in untempered deep cryogenic treatment. While tensile residual stress takes place in conventional heat treatment and shallow cryogenic treatment, compressive residual stress occurs in deep cryogenic treatment (Senthilkumar et al., 2011).

In a study where En 353 steel was used, the effect of shallow cryogenic treatment (-80 °C, 5 hours) and deep cryogenic treatment (-196 °C, 24 hours) on residual stress in comparison with conventional heat treatment, was examined. Results showed that tempering applied after deep cryogenic treatment, decreased the residual stress. The reason of this decline is associated with the amount of fine carbide precipitation which is more in deep cryogenic treatment (Bensely et al., 2008).

Bensely (2008), proved that when tempering is applied after deep cryogenic treatment, residual stress will decrease because of more fine carbide precipitation. However neither the types of carbides are identified and nor numerical measurement about the change in carbide content is made. For this reason it is not possible to establish a connection between the impact of sub-zero treatments on the micro structure of the material and mechanical properties like toughness and hardness, directly affected by micro structure. Besides, efforts to relate the effects of sub-zero treatments to the changes obtained about the wear resistance and fatigue, did not bear any results. Because as it is known, toughness, hardness and surface residual stress

can affect fatigue or wear resistance, therefore, these properties are controlled by other mechanical properties. For example, in both treatments while the values of toughness, hardness and compressive residual stress are exactly the same, with deep cryogenic treatment, rather than cold treatment, it is quite difficult to explain the 97% increase in the fatigue life.

In an other study, the impact of grinding/polishing process on the fatigue behavior of surface residual stress of AISI D2 steel produced by ingot metallurgy was examined (Sohar et al., 2008). There are also some studies about the measurement of residual stress on surface coating of AISI D2 steel (Huang et al., 2008; Imamura et al., 2007). It is seen that increasing TiN coating thickness, decreases residual stress (Imamura et al., 2007). As both the features and the effects of cutting performance of AlTiCrN/TiSiCN bilayer coating applied to AISI D2 steel was examined and as TiSiCN mono layer coating comprises high compressive residual stress, the cutting performance was affected negatively. The necessity of AlTiCrN layer where the stress had decreased was emphasized (Imamura et al., 2007).

Electrical discharge machining is a common method used both in processing metals and alloys and in die and space industries (Guu and Hocheng, 2001). This method causes tensile residual stress on the processed surface of the material (Guu and Hocheng, 2001; Guu et al., 2003). As EDM has a harmful effect on fatigue resistance, it is observed in the experiments that coating AISI D2 steel with TiN, either lessens the tensile residual stress or forms a compressive residual stress on the surface (Guu and Hocheng, 2001). Residual stress on AISI D2 steel, caused by LEHCPEB (low-energy high-current pulsed electron beams) a recently developed surface hardening method, is examined. This process changes the compressive residual stress on the surface layer of ferrite to tensile residual stress and this change is explained by phase transformations and deformations caused by heat stress (Zhang et al., 2013).

There is not any study in the literature examining the effects of cryogenic treatment on residual stress applied to AISI D2 tool steel. The unique importance of this study is that it examines the effects of deep cryogenic treatment in various holding times on residual stress which directly influences the service life of the material. In this study, in addition to the previous ones, residual stress, retained austenite, microstructure, toughness and surface roughness for various holding times between 0-24 hours is analyzed and optimum holding time is specified by analysing the relation of these parameters with residual stress. The reason for the usage of AISI D2 steel in industry is to improve the service life of the material under more economical conditions.

## CHAPTER 2

### DESCRIPTIONS

#### 2.1 Cryogenic Treatment

One of the main problems of conventional heat treatment composed of hardening and tempering is that it is soft and instable and moreover, in low temperatures it contains retained austenite ( $\gamma_R$ ) which turns into martensite having harder structure. To eliminate the retained austenite, either sub-zero treatments or multiple tempering processes are applied by holding the material under high temperatures for an extended period of time (Das et al., 2009c).

Applying sub-zero treatments to tool steels was first introduced by Scott in 1920 (Scott, 1920). Sub-zero treatments also gained recognition in industrial fields and they recently have a prominent importance in heat treatments of tool/die steels (Das et al., 2007).

Up to now, dry ice has been used as a means of cooling and it has been commonly named as cold treatment (193-223 K). With the help of the efforts in the last two decades, liquid nitrogen has been used as a means of cooling. Thus as the temperature decreased more, improvements in mechanical properties like wearing resistance are obtained (Bowes, 1974; Das et al., 2007; Carlson, 1990; Barron, 1982; Mohan Lal et al., 2001). This type of a sub-zero treatment is named as cryogenic treatment (77-193 K) (Bowes, 1974; Carlson, 1990; Das et al., 2009).

After applying cryogenic treatment at martensite finish temperatures below 0 °C to some steels like plain carbon steel containing more than 0.6% carbon, significant improvements were seen in some service features like toughness, fatigue life and wear resistance. It would not be right to relate these apparent improvements only with the increase in martensite in response to the decrease in retained austenite (Hotten et al., 2002). Following the cryogenic treatment, a notable increase is seen in



the service life of tools, punches, drill bits, end mills, bearings, cams, crank shafts and pistons (Baldissera and Delprete, 2008).

In a study carried out in Gh Asachi Technical University and in Louisiana Technic Institute in Romania it is stated that, in addition to the transformation of austenite to martensite, cryogenic treatment causes the following effects (Hotten et al., 2002):

- (i) Appropriate redistribution martensite carbide phases of alloy elements,
- (ii) Too much precipitation of alloy carbide elements with very small dimensions (smaller than 1  $\mu\text{m}$ ),
- (iii) Appropriate redistribution of residual stresses.

At the time of cryogenic treatment, a 4% increase in the volume of metal matrix is observed with the shift of retained austenite to martensite. The dilation of metal matrix, increases the dislocation density. Following this, the carbon atoms in the metal gathers round through dislocations and carbon rich regions are formed (Farhani et al., 2012).

## **2.2 Residual Stress**

Residual stress is defined as the stress system which occurs in an object when all the external forces are removed (Kafkas, 2001). Even if a machine element is produced without any residual stress, residual stress can be observed especially in service conditions where variable loading happens. For this reason a design engineer has to take all these types of stresses into account (Varol and Bedir, 1993). Residual stresses are elastic stresses. The maximum value of a residual stress is limited with the yield stress of the material. When the stress exceeds this value, unless there is a force in reverse direction, material deforms itself till the yield stress values is obtained. In other words, the value of residual stress decreases together with the plastic deformation (Varol and Bedir, 1993).

Changes in the volume is seen on the surface region of the work piece after the hardening treatments (Varol and Bedir, 1993). The main cause of the thermal based residual stress is the different dilations which happen when a metal is cooled

immediately after it is heated. In full or surface hardening processes, internal stress is induced as there are various temperatures in different parts of work piece. Because of that during this process, as a natural outcome, the cooling rate of outer surface regions is higher in comparison with inner regions. Besides residual stress is also observed as a result of phase transformations (Dülek, 2002; Kafkas, 2001, Varol and Bedir, 1993).

Stress on the material is described as normal stress vertically affecting the surface and shear stress affecting the surface in a parallel manner (Figure 2.1). If the sign of the normal stress is negative it is defined as compressive stress and if it is positive than it is defined as tensile stress. Compressive residual stress tries to push the material whereas tensile residual stress forces the material to separate by pulling it (Skalli and Flavenot, 1985).

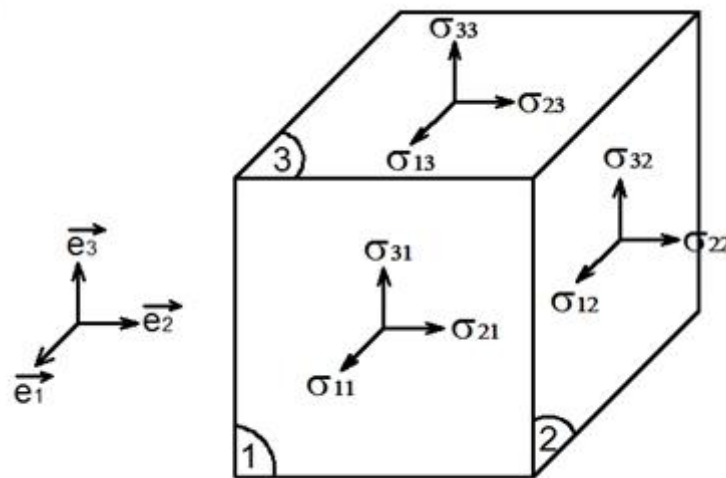


Figure 2.1. Stress components in a material.

Generally, residual stresses are classified into three in accordance with greatness of the affected area:

1. Order (Macro) Residual Stress

This type of residual stress affects greater areas on the material and causes dimensional changes (Withers and Bhadeshia, 2001a). They appear as a result of many thermo mechanical and mechanical processes including machining, welding, heat treatment and coating as (Hanabusa et al., 1985; Macherauch, 1987).

## 2. Order (Micro) Residual Stress

Covers one piece or a part of a piece and are formed between different phases. They appear as a result of deformations caused by biphasic materials having both different yield point and work hardening (Hanabusa et al., 1985; Macherauch, 1987). Furthermore, they can be formed during heat treatments due to uncompleted transformation of two phases with different specific volumes (Macherauch, 1987).

## 3. Order (Micro) Residual Stress

Effective in several atomic distance within the piece and are balanced in a tiny part of the piece (Lu, 1996). They appear as a result of structural deformations including dislocations (Macherauch, 1987). First fatigue cracks, seen in machine elements subjected to variable loads, originates from this type of stress in crystals (Withers and Bhadeshia, 2001b). Macro and micro stresses are shown in Figure 2.2.

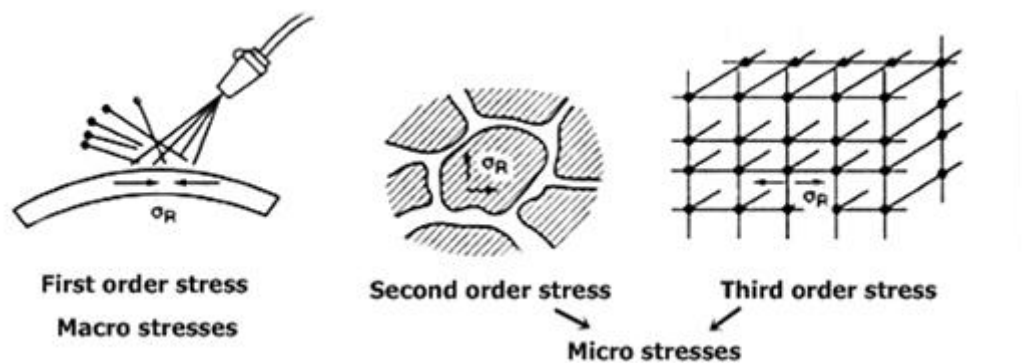


Figure 2.2. Different kinds of residual stress (Skalli and Flavenot, 1985).

If impact areas of residual stress are described dimensionally, the following approach is accepted (Withers and Bhadeshia, 2001b):

- 1. Order residual stress impact area  $\approx$  dimensional size of the material
- 2. Order residual stress impact area  $\approx$  3-10 $\times$  average piece size
- 3. Order residual stress impact area  $<$  average piece size

In order to demonstrate the link between these three groups of residual stress, let us assume a plate which is plastically deformed. When the loading is over, deformation toughness of a piece, in comparison with the other one, and deformation toughness of the surface (in comparison with the inside) will form a micro stress system together with nonhomogeneous yielding and dislocation yielding. Simplified schematic view of the residual stresses is given in Figure 2.3. Continuous lines with frequent oscillation signify second and third degree residual stresses. Dotted lines between a-b and c-d signify compressive stress, and between b-c they signify macro stresses with tensile stress (Lu, 1996).

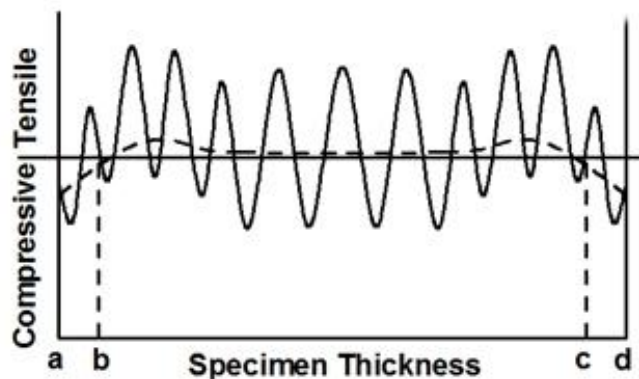


Figure 2.3. Macro stresses in a layer (continuous lines) and micro stresses (dashed lines) (Lu,1996).

Formation of residual stresses results from (Lu, 1996):

- (i) Plastic deformation or forming including rolling, drawing, extruding, bending, forging, pressing, shot peening ve laser shock.
- (ii) Welding, coating (electro deposition, PVD, CVD), and machining.

- (iii) Quenching, laser and plasma heat treatment, case hardening, ion plating, and combinations of these treatments, casting, and cooling of multiphase materials.

### 2.2.1 The effect of residual stress on working performance

Tensile residual stress decreases the working performance of the materials. However, it is known that the fatigue life of compressive residual stress has beneficial effects on crack propagation and stress corrosion. In fact, residual stress can be taken as static loads in elastic range. Residual stress relaxes in the elastic range (Lu, 1996). Superposition rule of various stresses can be defined as follows:

On a stress plane, if a material specimen imposed residual stress defined with  $\sigma_R$  vector is considered and if the imposed stress on the same point of the plane is superposed with  $\sigma_A$  the real stress  $\sigma_N$  imposed on the specimen is shown with the following vector:

$$\sigma_N = \sigma_A + \sigma_R \quad \text{Equation 2.1}$$

In Figure 2.4, collision of residual stress and stress imposed to the material in bending fatigue test with the material the surface of which was previously hardened or shot peened, is given.

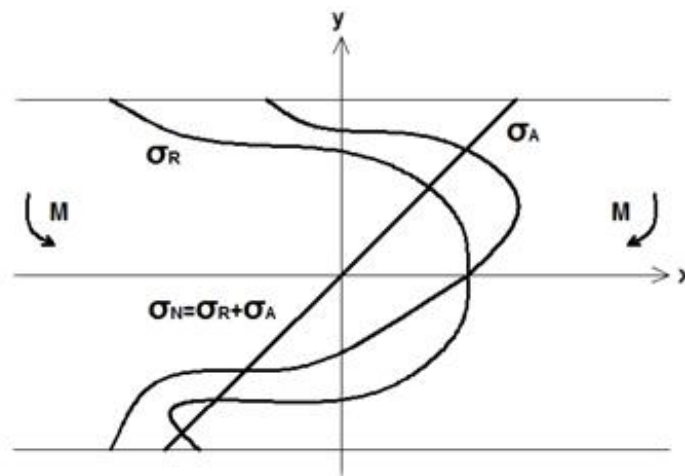


Figure 2.4. Superposition of residual stress and applied stress (Lu, 1996).

$\sigma_A$  stress distribution occurs in the particle exposed to bending moment. This stress should be added to the already existing stress of  $\sigma_R$  particle. Thus, the real stress distribution of the particle  $\sigma_N$  is the sum of these two residual stresses.

Residual stress can be relaxed with heat and mechanical treatments. The relaxation in residual stress is in relation with many complex interactions like amplitude, heat, initial residual stress, the structure and mechanical properties of the material (Lu, 1996).

Induction hardening process can cause compressive residual stress which improves the fatigue strength of mechanical parts. Residual stress is extremely important for stress corrosion. Compressive residual stress caused by shot peening can notably increase the stress corrosion behaviour of the processed material (Lu, 1996).

The performance of the material which went through heat treatment, mechanical treatment and other loading types is in relation with the residual stress formed during the production method. In some cases parts consisting the least residual stress are better. In other cases to improve the mechanical behaviors like fatigue compressive residual stress is needed on the surface of the material. For this reason the measurement of residual stress is quite significant. The level of residual stress, in proportion to the load applied, is important. Being aware of the residual stress situation of the material provides convenience for stress analysis in mechanical particle design. As a result, residual stress behaves like an average stress and effects the mechanical properties of the material like brittle fracture, fatigue, stress and fatigue corrosion (Lu, 1996).

### **2.2.2 Measurement Methods for Residual Stress**

These methods, also called as mechanical methods, depend upon measuring the deformations of the material during or after stress which is done on purpose by removing the material to allow stress relaxation (Rithers and Badeshia, 2001). In

these methods, first a new stress is created by removing the material from the piece analysed and then by measuring the displacements, local change in the stress is identified. Finally, residual stresses are calculated with the help of elasticity theory (Ekmekci, 2004). These measuring techniques are sensitive to macro residual stresses.

The process is finalized as follows (Lu, 1996):

- (i) Formation of stress by processing or layer removal,
- (ii) Determining the local change in the stress by measuring the deformations or displacements,
- (iii) Calculating the residual stress by elastic theory as a function of measured deformation (analytical approach or finite element calculations).

Most widely used destructive methods can be defined as follows:

- Layer Removal method
- Hole Drilling method
- Ring Core method
- Sectioning method
- Crack Compliance/Slitting method
- Contour method

The second series of these methods are non-destructive methods. These depend on physical or crystallographic parameters and the relation of residual stresses. Most widely used non-destructive methods are as follows:

- X-Ray diffraction method
- Neutron diffraction method
- Ultrasonic method
- Magnetic Barkhausen Noise method
- Raman Spectrum Method

X-ray diffraction and neutron methods, by looking for the changes between the planes of polycrystalline materials, depends on lattice deformation measurements.

The first method measures the residual deformation on the surface of the material and the second one measures deformations in the volume. Diffraction methods also search for the three groups of residual stress (macro and micro stresses) (Lu, 1996).

### ***2.2.2.1 Non-destructive Methods of Residual Stress Measurement***

#### **2.2.2.1.1 X-Ray Diffraction (XRD) method**

When a monochromatic X-ray irradiates on a solid material, it is scattered by the atoms forming the material. For a perfect crystal material, atoms are scattered regularly on three dimensional periodic lattice. The distance between the crystallographic planes are determined perfectly. Scattered waves, because of the regular scatter of atoms, cause mutual interaction similar to visible ray diffraction due to the optical diffraction pattern (Lu, 1996).

When wavelength  $\lambda$  is constant, atoms in a certain plane cause to diffraction of incident beams. Diffracted beams intersect and make indentation on the film around the specimen. The planes of which spacing carries out Bragg's law, radiation cone sections the film. When  $2\theta$  is calculated analysing the film, spacing of interplanar can be determined. If specimen is bended about  $\psi$  angle, atomic planes also bend about  $\psi$  angle. In the event that there is no residual stress in material, both of diffracted beams coincide (Asi and Can, 2001). If there is residual stress in material, atomic planes at different directions contract or expand and peak value changes (Figure 2.5).



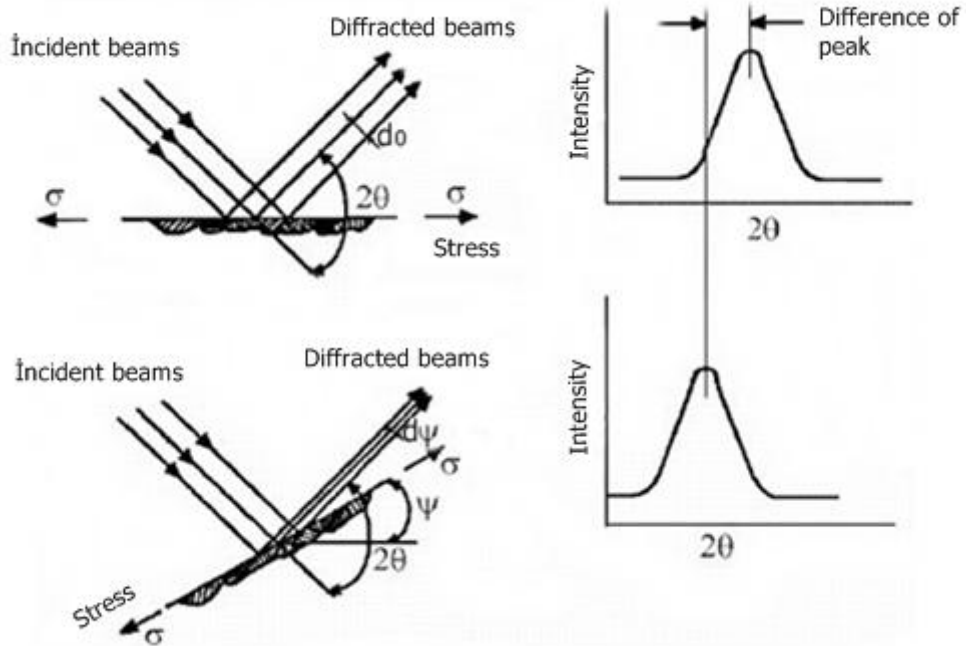


Figure 2.5. Determination of residual stress using X-ray diffraction method (Asi and Can, 2001).

The summit angle of the cones are as follows in Equation 2.2:

$$\alpha_i = \pi - 2\theta_i \quad \text{Equation 2.2}$$

$\theta_i$  diffraction angle is in relation with Bragg's law lattice spacing. If these angles are measured with an appropriate instrument, it will be possible to find out lattice spacing of crystallographic planes 'd' (Lu, 1996).

Bragg's Law is shown with Equation 2.3:

$$n\lambda = 2d\sin\theta \quad \text{Equation 2.3}$$

$D$  is the distance between diffraction lattice planes,  $\theta$  is incident ray and angle between the diffraction plane,  $\lambda$  is the wave length of X-ray and  $n$  is an integer in Figure 2.6. When the Bragg law is applied, diffraction ray and incident ray lattice plane is symmetrical. Infinite crystallographic plane is determined, nonetheless only

few of them forms diffraction model which is dense enough to be detected (Lu, 1996).

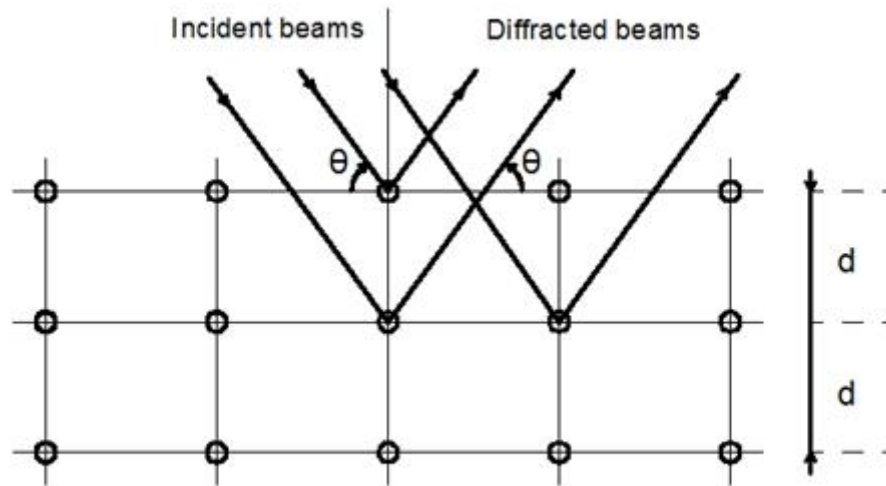


Figure 2.6. Planes carrying out Bragg's Law (Lu, 1996).

#### 2.2.2.1.2 Neutron diffraction method

The physical principles of X-ray diffraction and neutron diffraction methods are similar. X-rays provide the measurement of stresses several microns away from the surface, whereas the importance of neutron diffraction lies in the fact that it can detect residual stresses through the thickness of steel pieces. The penetration of neutrons is 1000 times greater than the penetration of X-rays. Thus a measurement of 4-50 mm penetration depth can be done. Besides deflections, measurement can also be done in transmission of neutrons. Therefore, a stretch component can be measured by positioning as demanded in the specimen through angle bisectors of incident and scattered rays.  $\sin^2 \psi$  method can be used in detecting non-normal strain components in X-ray method but it is not preferred in neutron diffraction method. This technique can only be practiced in a laboratory environment and the instruments used are quite expensive (Yelbay, 2008).

#### 2.2.2.1.3 Ultrasonic Method

These methods benefit from sensitivity of stress levels on material to velocity of ultrasonic waves moving through a solid material. The direction and magnitude of already existing residual stresses directly affect the change of the velocity of ultrasonic waves (Yiğit et al., 2008).

The advantages of this method is that the equipment is practical, portable and can easily be installed. Moreover the cost of the method is low and it does not have any radiation damage. Besides, by ultrasonic method macro residual stresses can be found independently with the depth of the material. Furthermore, as the velocity of sound changes according the direction in nonisotropic materials, distinguishing flight distance taken from this region is substantially hard. In addition, as velocities of sound varies in regions with microstructural changes, measuring the differences in these regions is quite difficult (Yelbay, 2008).

Ultrasonic methods used for stress measurement are related to changes in wave velocity, which can be defined with the following relation in Equation 2.4:

$$V = V_0 + K\sigma \quad \text{Equation 2.4}$$

$V_0$ , wave velocity in a stress free medium,  $\sigma$  stress and  $K$  a parameter related to material.

#### 2.2.2.1.4 Magnetic Barkhausen Noise Method

Barkhausen noise is the sound signal occurring as result of the movement of magnetic dipoles or their orientation in ferromagnetic materials. As it is seen in Figure 2.7, ferromagnetic materials consist of small regions in which magnetic dipoles are formed. These regions are called as domain.

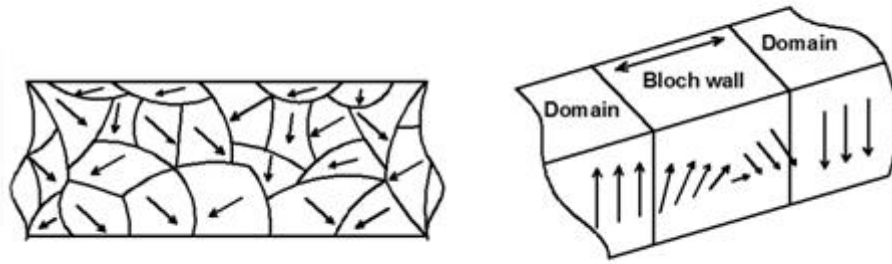


Figure 2.7. Domains and magnetic dipoles in a ferromagnetic material (Yelbay, 2008).

Before magnetization, ferromagnetic materials are oriented disorderly in magnetic dipoles and domains (Figure 2.8). At this moment net magnetic field strength is zero. When an external force or magnetic field is exerted, magnetic dipoles, which were oriented disorderly, start turning towards magnetic field or the exerted force. Movement happens as the walls of domains move.

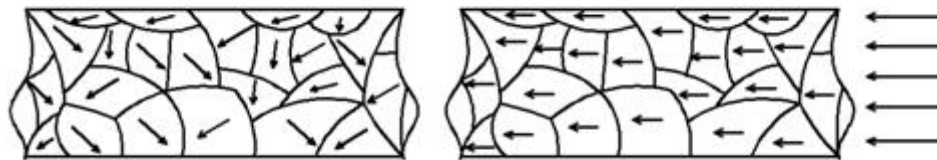


Figure 2.8. Orientation of domains in a scattered situation (left) orientation of domains according to magnetic field (right) (Yelbay, 2008).

The importance of Barkhausen method has increased recently as it can be easily used, as it is fast and portable. When compared with other known non-destructive residual stress measurement methods, it is seen that Barkhausen method gives accurate results (Yelbay, 2008).

#### 2.2.2.1.5 Raman Spectrum Measurement Method

Raman spectrum measurement method finds residual stress by measuring the interaction of laser beams with the material. Laser beams sent to the material causes the atoms to oscillate. By analysing the scattered rays, it is possible to find out about the chemical and physical structure of the material. In Raman spectrum measurement method, resolution is very high and it is generally used in measuring the surface residual stress. Nowadays, studies about Raman spectrum measurement method, are mostly about its usability on composite materials (Yelbay, 2008).

#### ***2.2.2.2 Destructive Methods of Residual Stress Measurement***

##### ***2.2.2.2.1 Layer Removal Method***

The principle of layer removal method is simple. A plane with a residual stress is deformed to preserve the balance of static moments and internal forces. Deviation is related with the magnitude and type of residual stress distribution throughout the thickness of material. If the layers of the material containing residual stress are removed with a chemical treatment, then balance of internal stress and moments will immediately be broken. To establish this balance, the particle has to deform. The variance in deviation produced by the removed layer, is associated with surface stress of the removed layer (Figure 2.9).

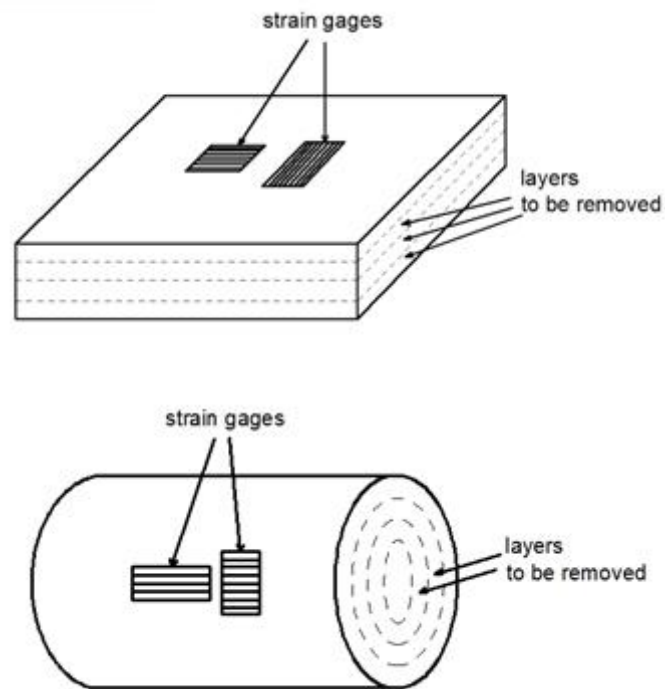


Figure 2.9. Layer removal from a rectangular component (above) Layer removal from a cylindrical component (below) (Treuting and Read, 1951).

#### 2.2.2.2.2 Hole Drilling Method

Hole drilling method is a semi-destructive residual stress measuring method which is sensitive to 1. Order macro residual stress.

##### 2.2.2.2.2.a Hole Drilling Method via Strain Gages

Hole drilling is a convenient and effective method in measuring residual stress. The main principle of the method was first developed by Mathar in 1934. Since then, many researches developed this method and in the end it was standardized with ASTM E837 code (Schajer, 2006). The real and the most prevalent objective of hole drilling method is calculating uniform residual stress in assumed plane, either from surface to the depth of a thick material or through the thickness of a thin material (Schajer, 2001).

The application principle of hole drilling method is quite simple. A tiny hole is drilled on the material and after drilling free deformations appear and these are measured with strain gages. Afterwards, it is possible to measure the initially existing residual stresses around the hole by means of a series of calculations (Lord, 2002). The diameter of the hole is about 1.8 mm and the depth is about 2 mm. When compared with other residual stress measuring techniques, hole drilling method can be apply for all material types generally (Rossini et al., 2011). Schematic three dimensional view of this method is seen in Figure 2.10.

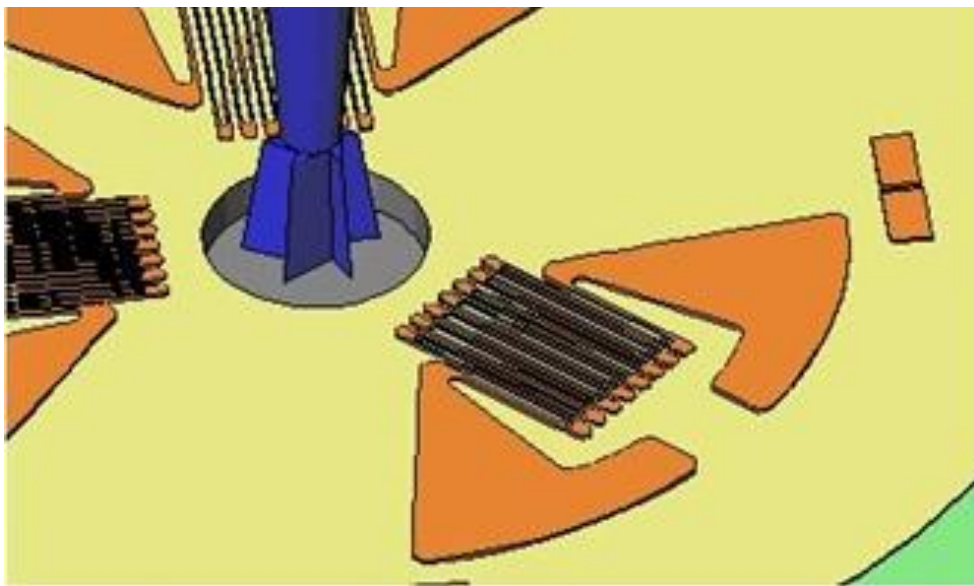


Figure 2.10. Three dimensional view of hole drilling.

These steps are followed in measurement (Vishay, 2007):

1. Three or six-element strain gages are placed on test material where the residual stress will be measured.
2. Strain gages are tied to a unit deformation indicator with cables.
3. Drilling apparatus is placed to the center of strain gages.
4. After the unit deformation values are set to zero, a hole is drilled in the geometric center of strain gages.
5. Free deformations corresponding to the initial residual stresses are read.
6. Special data reduction correlations and principal residual stress and their angular orientations are measured from the stretches.

In this method the measurement precision changes in accordance with the depth of drilling. As the depth increases, the precision decreases. As it is seen in Figure 2.11,  $D$  is diameter of strain gages, and  $D_0$  is the diameter of the hole to be drilled. According to ASTM E837 standart  $D_0$  must be between  $D_0 = 0,3 - 0,5 D$  and the maximum depth must be  $Z = 0,4 D$  (ASTM E837; Lord, 2000). As the proportion of the diameter of the hole to be drilled to the diameter of strain gages  $D_0/D$  increases, the precision  $(D/D_0)^2$  increases as well (Grant et al., 2002).

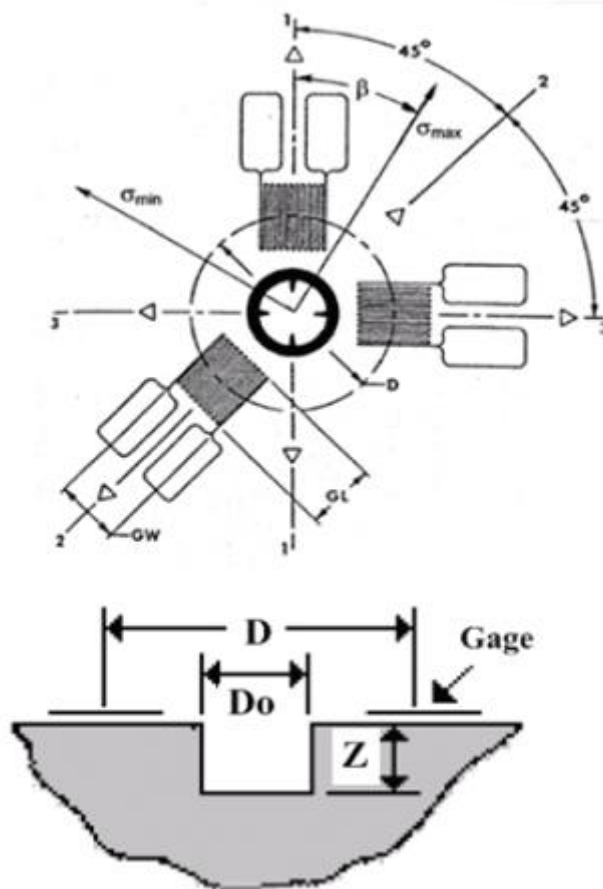


Figure 2.11. Schematic view of strain gages (Lord, 2000; Vishay, 2007).

In Figure 2.12, the radius of hole is shown with  $R_0$  and the radius of strain gages is shown with  $R$ . In a uniaxial loading, transformation of relieved stress is seen from the distance to the hole surface. As it is seen in the figure, the relieved stress decreases as we get further from the hole. For this reason strain gages must be placed closer to the hole.



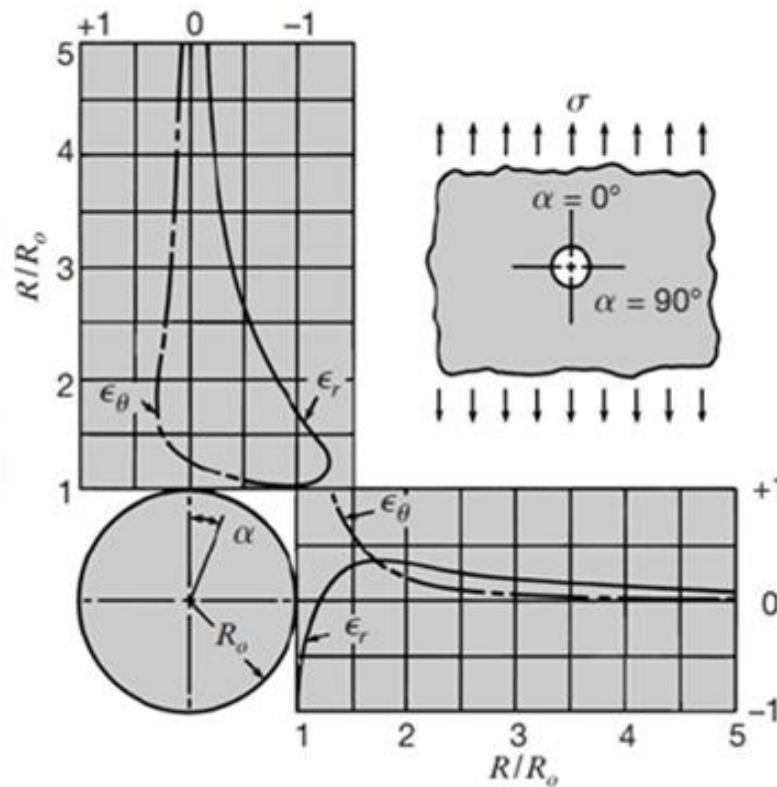


Figure 2.12. Variation of tangential and axial strains relaxation moving away center of the hole (Lord, 2000; Vishay, 2007).

Benefits of hole drilling method in comparison with other methods are as follows (Schajer, 2001):

- Damage on the material is rather slight.
- Accepted both experimentally and theoretically.
- Application of the method is simple, fast and cost effective.
- Results are reliable.
- Needs less special equipment.
- Measuring installation is portable.

Disadvantages of the method are as follows (Lord, 2008):

- Stresses close to the surface can be measured.
- Measurement sensitivity decreases in proportion with depth.
- Measurement area is limited.

#### *2.2.2.2.2.b Residual Stress Measurement with ESPI (Electronic Speckle Pattern Interferometer)*

Basic steps of stress measurement with ESPI technique are as follows:

- (i) Starts with imagery recording, controlling the convenience of the surface for hole drilling.
- (ii) A laser sent to the piece is viewed with CCD (Charge-Coupled Device) and the integration of reference and reflected beam is provided on the prism point while passing through the lens system.
- (iii) At this moment the image is recorded in a camera and transferred to the computer for processing. This first image resembles to an interference pattern formed by illuminated and non-illuminated points formed randomly by surface roughness and optical mechanisms.
- (iv) To identify the position of each piece, four images both before and after hole drilling are taken and studied.
- (v) These four images are characterized with the phase transformations of reference beam in  $0^\circ$ ,  $90^\circ$ ,  $180^\circ$  and  $270^\circ$ . At least one set imagery is taken when all hole drilling steps are completed (Figure 2.13). The software shows the instant fringe images by calculating the set, recorded before hole drilling, with the instant real images. Fringe images define the displacements occurred due to hole drilling process (Schajer and Steinzig, 2005).

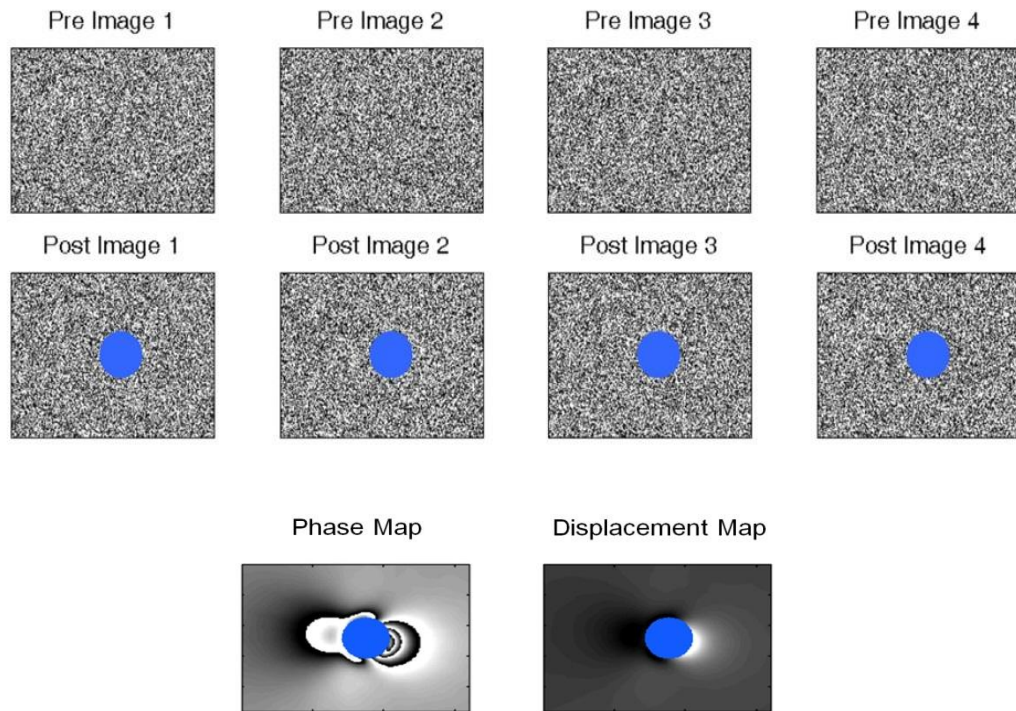


Figure 2.13. Determination of displacement map (Stresstech Oy., 2013).

The schematic view of hole drilling with ESPI method is given in Figure 2.14.

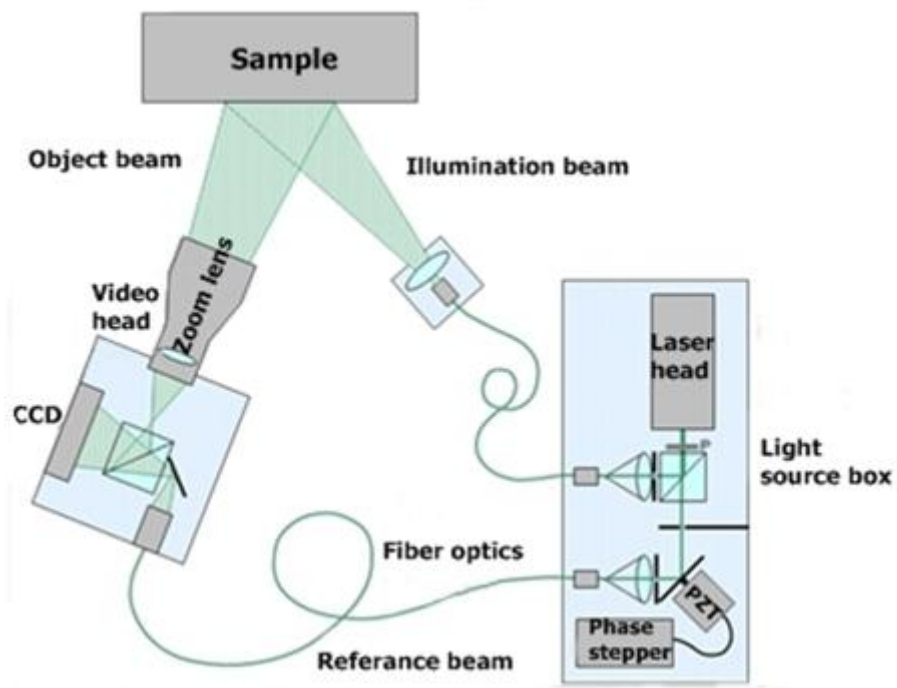


Figure 2.14. Schematic view of the ESPI system (Stresstech Oy., 2013).

In Figure 2.15. interference pattern around the hole, formed as a result of hole drilling is shown. The size of interference area is in proportion with stress relief.

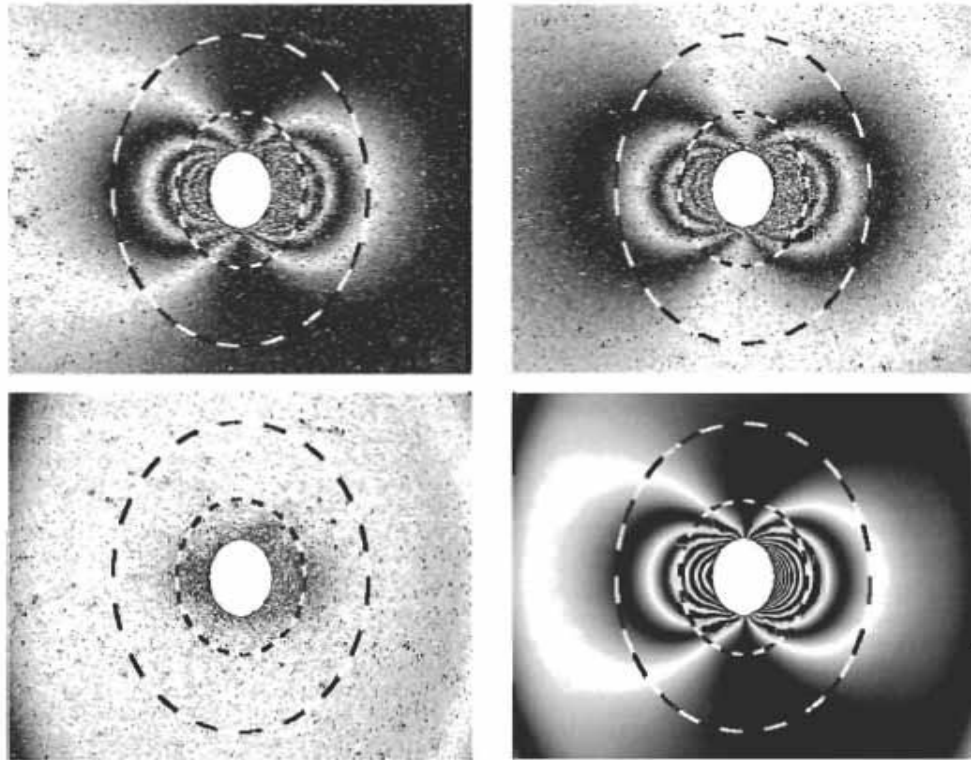


Figure 2.15. Fringe patterns (Stresstech Oy., 2013).

Surface preparation is not necessary as positioning strain gages is not used in this technique. Surface displacements directly proportional with the hole depth.

Benefits of ESPI technique in comparison with strain gages are as follows (Focht ve Schiffner, 2003):

- It's a non-contact method,
- It measures the whole area,
- It has high sensitivity ( in dimensions below micrometer),
- Various hole diameters can be used,
- Errors, arising from incorrect centered strain gages and the hole, do not occur.

### 2.2.2.2.3 Ring Core Method

Ring core method is a variation of hole drilling method. In this method, strain gages with three-element which are seen in Figure 2.16 measure the stress relief on the surface of the material in the ring. Similar to hole drilling method, residual stress existing before the ring core is drilled can be calculated with the measured relieved stretch. This method is also frequently named as semi-destructive method. Removed material is limited and the damage on it can adequately be repaired (Lu, 1996)

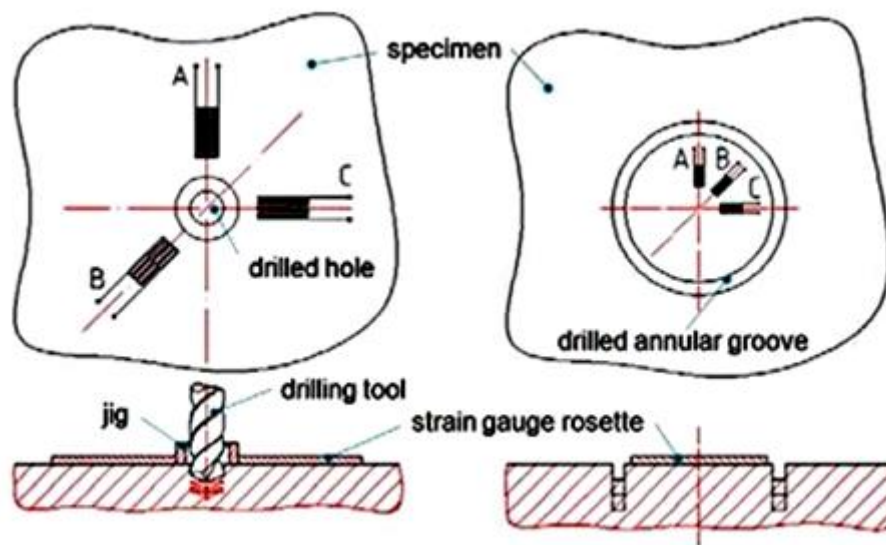


Figure 2.16. Hole drilling method (left) and ring core method (right) (Sarga and Menda, 2013).

Just like the hole drilling method, ring core method is practical and fast. It is used less frequently despite of the fact that it provides greater surface stretches in comparison with hole drilling method (Rossini et al., 2012). It is less convenient and damages the material more. To drill the ring, strain gages must be untied and tied again. However, in hole drilling method, ties do not get any damage from drilling process (Lu, 1996).

#### 2.2.2.2.4 Sectioning method

Sectioning method is a destructive residual stress measuring method based on removing material from the specimen (Shadly et al., 1987; Tebedge et al., 1973). This method is mainly used to analyse the residual stress in structural carbon steel, stainless steel and in aluminum materials.

Residual stress within the specimen, is measured by removing sections from the specimen. To identify the residual stress, the specimen is cut sequentially in various section (Figure 2.17). The method provides great elasticity in determining the details of residual stress through the related area by uniting separation, slitting and layer removing processes. Relieved stretches, during cutting processes, are generally measured by using electrical or mechanical strain gages (Schajer, 2001; Yiğit et al., 2008).

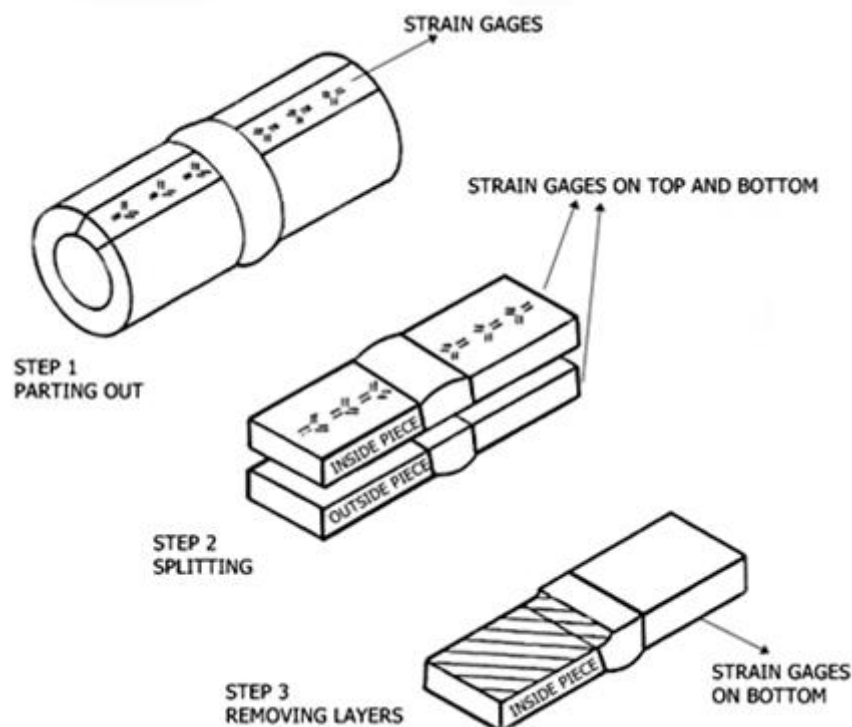


Figure 2.17. Schematic view of sectioning method (Lu, 1996).

#### 2.2.2.2.5 Slitting or crack compliance method

The general principle of this method is to open fractional slot on the surface of the material and to measure the changes around the slot as a function of slot depth. Free transformations, vertical to the slot, are measured with strain gages placed near the slot (Figure 2.18). Slots are cut gradually by using a processing cable with electrical discharge machining. Measured transformations are used for calculating residual stress before the slot is opened (Rankin et al., 2003).

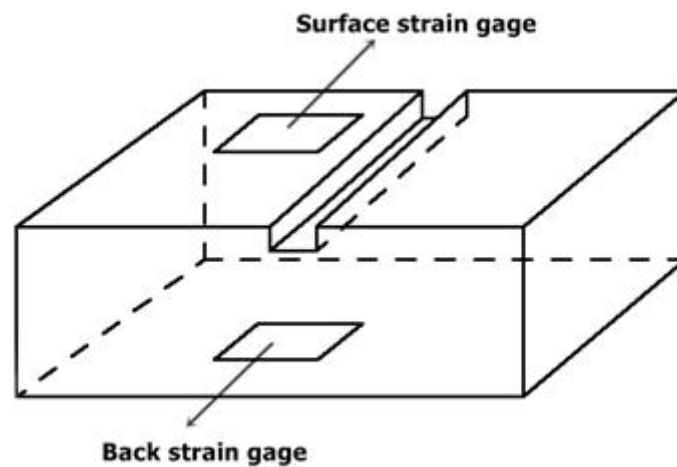


Figure 2.18. Schematic view of slitting or crack compliance method (Prime, 1999).

Application of the method is simple and fast and it is especially very sensitive in measuring regional residual stress. Furthermore, residual stress in specimen with varied geometrics can be measured. The method has a beneficent depth stress resolution and sensitivity. It can be easily applied to the non-crystalline structure specimens. However, this method can measure residual stress vertical to slot direction and unit deformations and the slots do not have any standard order (Yiğit et al., 2008).

#### 2.2.2.2.6 Contour method

In this method, measured displacements are used in estimating the residual stress. On the contrary, the principle of measurement in multi-axis incision profile is based on calculating specific stretches with measured displacements and then residual stress is subtracted from specific strains. The source of all residual stresses are in harmonic stretches on a material. Many researches studied residual stress in engineering particles by using the specific stretches (Ueda et al., 1986; Hill, 1996). Specific stretches are preferred in this method as they remain constant with the re-distribution of residual stresses. In other words, the change in the geometry of a particle also causes a change in residual stresses but it does not affect specific stretches. Besides, as long as specific stretch distribution is known, residual stress of each structure divided from the particle, can be calculated.

Although the method is a destructive one, the application is quite easy and residual stresses in all incisions can be measured in a short period of time with an appropriate cost (Figure 2.19). However, in this method residual stresses vertical to slitting plane can be measured (Zhang et al., 2005).

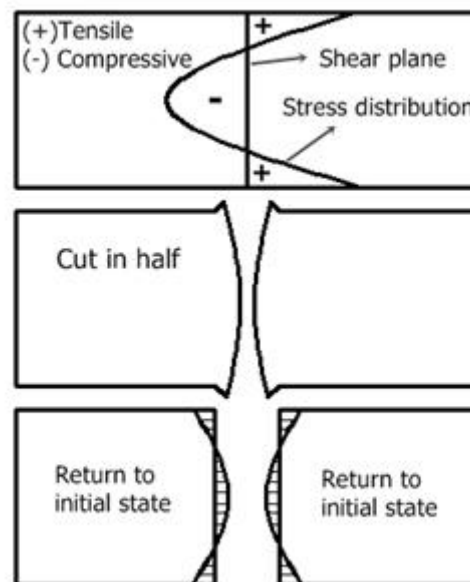


Figure 2.19. Schematic view of contour method (Lu, 1996).



### 2.2.3 Comparison of Residual Stress Measurement Methods

In Table 2.1, destructive and non-destructive residual stress measuring methods are compared in accordance various parameters.

Table 2.1. Comparison of residual stress measurement methods (Yiğit et al., 2008)

Method		Kind of stress	Penetration depth	Measurement speed	Destruction rate	Equipment cost	Application
Destructive Methods	Layer Removal	Macro	10-500 $\mu\text{m}$	Fast	Destructive	Low	All kinds of materials if geometry conditions carry out
	Hole Drilling			Medium	Semi destructive	Low	
	Ring Core		100 $\mu\text{m}$ -6 mm	Medium	Semi destructive	Low	
	Sectioning		8-100 mm	Medium	Destructive	Low	
	Crack Compliance/ Slitting		150 mm	Medium	Semi destructive	Low	
	Contour		-	Fast	Destructive	Low	
Non-destructive Methods	X-Ray diffraction	Micro and macro	<50 $\mu\text{m}$ (Al) <5 mm (Ti)	Slow	Non-destructive	Medium	Materials with crystal structures
	Neutron diffraction			Very slow		High	
	Magnetic Barkhausen Noise	Macro	>100 mm	Very fast		Low	Mono phase material
	Raman Spectrum Measuring	Micro and macro	6-10 mm	Very fast		-	Ferromagnetic materials
	Taman Rayf	Macro	<1 $\mu\text{m}$			-	Polymeric composites

## CHAPTER 3

### Experimental Procedures

#### 3.1 Materials

AISI D2 involving high carbon and chrome is a cold tool work steel which has high wear resistance, compressive strength and toughness, dimensional stability in heat treatment, compatibility for surface treatments such as PVD, nitriding. Blanking dies up 6 mm thickness requiring toughness, crushing dies, spinning dies, drawing dies, cold extrusion dies, dies used for manufacturing of aluminum and zinc tubes, drilling-inflating dies for manufacturing of bolt, nut, fastener (Assab & Korkmaz). Chemical composition of AISI D2 steel is seen in Table 3.1 and physical properties are shown in Table 3.2.

Table 3.1. Chemical composition of AISI D2 steel (Assab & Korkmaz)

ISO/DIN	AISI	%C	%Mn	%Cr	%Mo	%V	%Si
1.2379	D2	1.55	0.4	11.8	0.8	0.8	0.3

Table 3.2. Physical properties of AISI D2 steel (Assab & Korkmaz)

Temperature	20 °C	200 °C	400 °C
Density (kg/ m <sup>3</sup> )	7700	7650	7600
Thermal expansion coefficient	-	12.3 * 10 <sup>-6</sup> 11.2 * 10 <sup>-6</sup>	12 * 10 <sup>-6</sup>
Thermal conductivity (W/m °C)	20	21	23
Modulus of elasticity (MPa)	210000	200000	180000
Specific heat (J/kg °C)	460	-	-

AISI D2 steel is a certificated steel and was obtained from Assab Steel Company. Specimens are turned into cylindrical parts which have 20 mm diameter and 50 mm length (Figure 3.1).



Figure 3.1. Dimensions of specimens.

Austenization and tempering treatments, named as conventional heat treatment, were applied but cryogenic treatments were not applied to the specimens in the first group. Austenization, cryogenic treatment in various holding times and tempering were applied respectively to the other specimen groups (Table 3.3).

Table 3.3. Treatments applied to specimens

Specimen	Austenization	Cryogenic treatment at -145°C	Tempering
1	1030°C 30 min	Not applied.	525°C 2 h
2		30 min	
3		4 h	
4		16 h	
5		24 h	

Specimens to be used in the experiments have classified regarding heat treatment seen in Figure 3.2.



Figure 3.2. Classification of specimens before treatments.

Before the austenization process, preheating was applied to the specimens (respectively 650°C, 850 °C). Specimens were put into the furnace preheated at 650°C. After temperature of specimens reached at 650°C, furnace was heated up to 850 °C and specimens were held at 850 °C for 20 min. Then austenization was carried out at 1030°C by holding the specimens for 30 minutes. For quenching, specimens were kept till 60°C in a 3-bar vacuum furnace. Finally, specimens were left in the air to attain room temperature (25°C). Tempering for two hours at 525°C were applied to the specimens in the first group. The steps of conventional heat treatment are given in Figure 3.3.

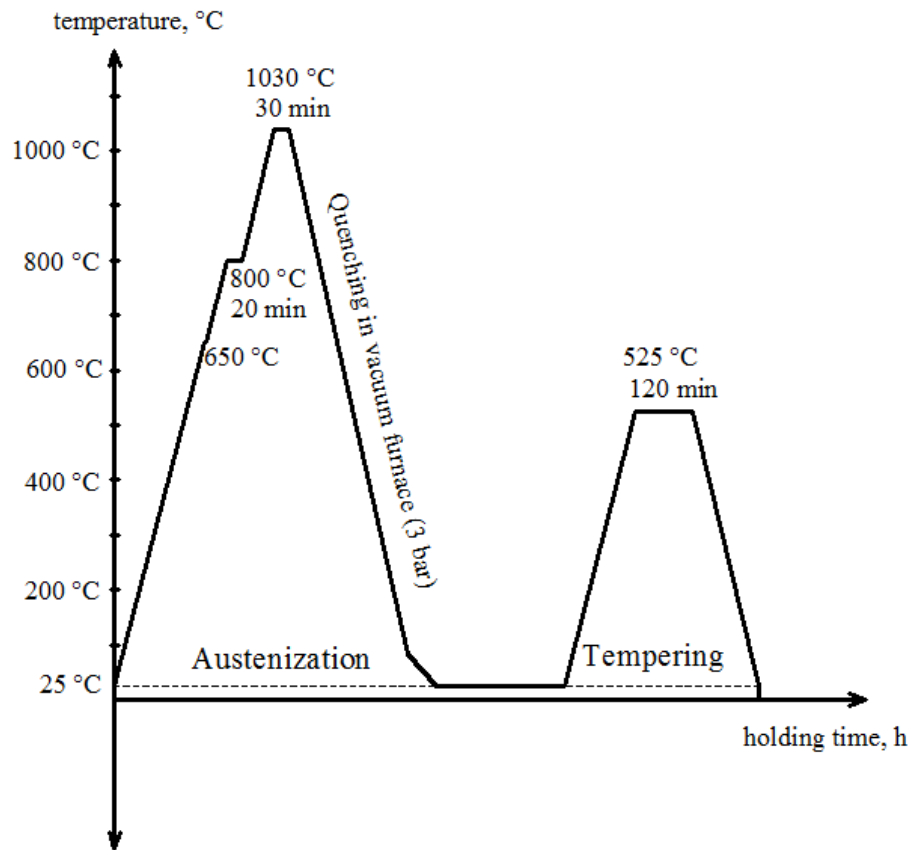


Figure 3.3. Conventional heat treatment (austenization+ tempering).

Cryogenic treatment at  $-145^{\circ}\text{C}$  was applied both to the specimens going through the process of deep cryogenic treatment in Alper Heat Treatment Company and to the specimens which were held till the room temperature following. The furnace for cryogenic treatment is seen in Figure 3.4.

The holding time in cryogenic treatment ( $t_{CT}$ ) were set as (30 min, 4, 16 and 24 hours). Specimens were kept in cryogenic heat for the established time period, were taken out of cooling oven and kept outside till the room temperature. As a last step two hours tempering at  $525^{\circ}\text{C}$  was applied to the specimens. Finally, specimens were left in the air to attain room temperature ( $25^{\circ}\text{C}$ ).



Figure 3.4. Cryogenic treatment furnace (above) and temperature-pressure indicator (below).

Figure 3.5 represents that combination of cryogenic treatment and conventional heat treatment. After austenization, specimens were exposed to cryogenic treatment and tempering.

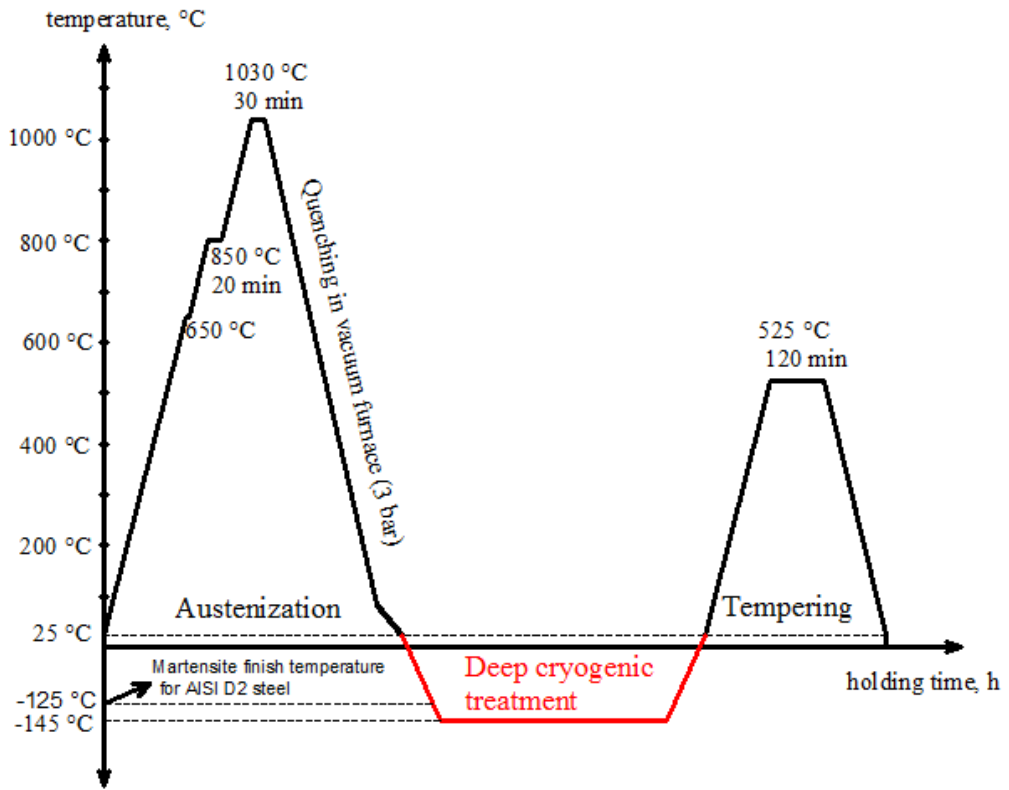


Figure 3.5. Austenization+cryogenic treatment+tempering.

Holding times at cryogenic temperature is detailed in Figure 3.6. It can be seen various holding times at cryogenic temperature.

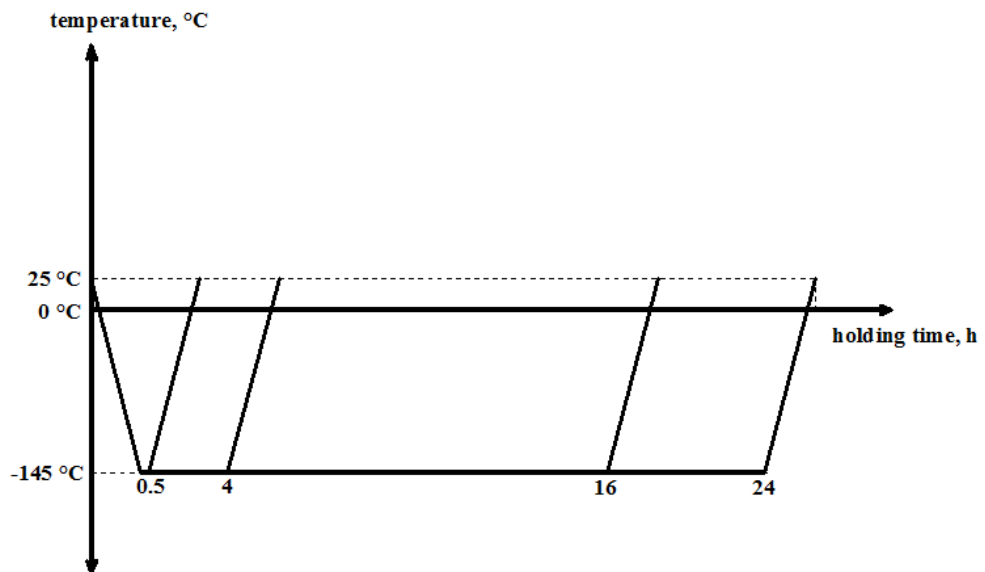


Figure 3.6. Cryogenic treatment at various holding times.

When tempering temperature (525 °C) is selected, the graph in Figure 3.7 is used.

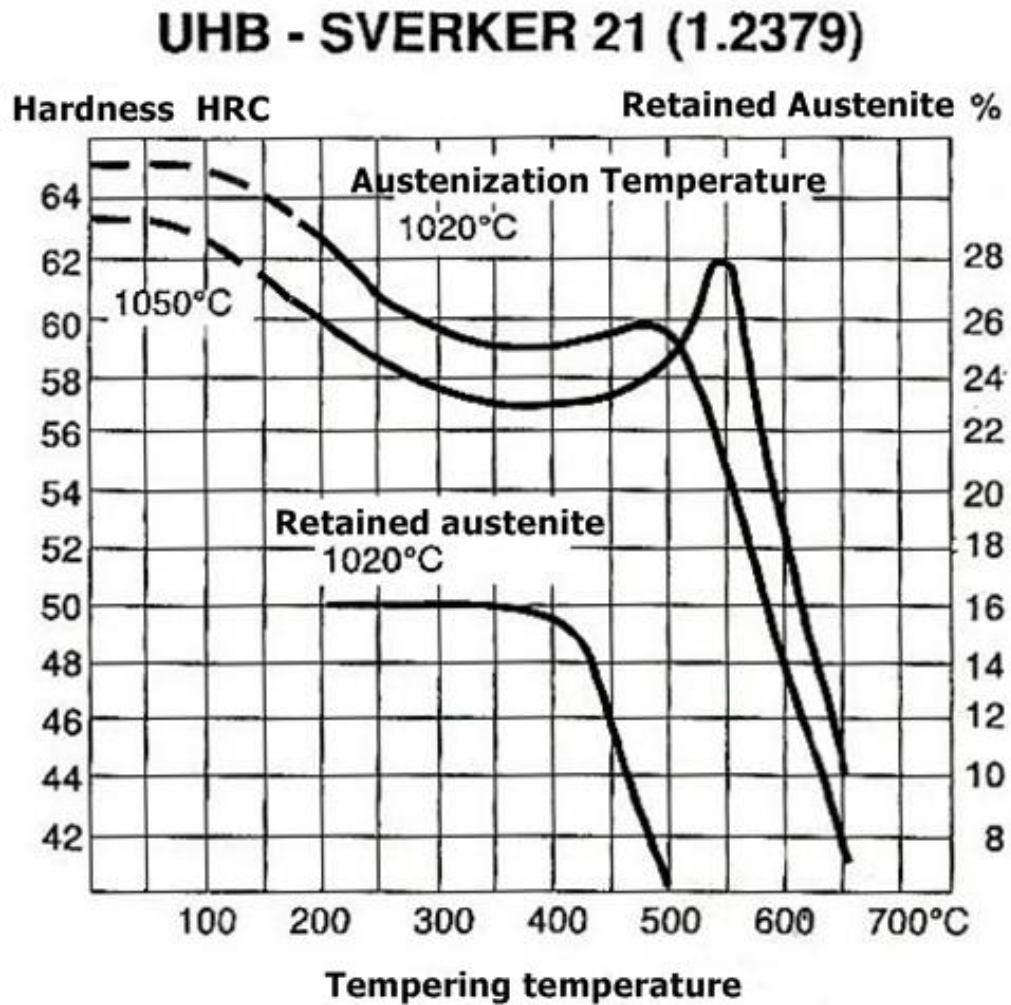


Figure 3.7 Selection of tempering temperature (Assab Korkmaz).

### 3.2 Measurement of Residual Stress

Among the all residual stress measuring methods, X-ray diffraction method is a more special one. Because, this method provides possibility for non-destructive measurement of residual stress on the material's surface, which is necessary in estimating the fatigue life of materials. When compared with other conventional methods, X-ray diffraction enables real time analysis and local measurement of stress formation. In addition, depth graphic of stresses can be obtained with electro polishing technique (Lu, 1996).



Residual stress on the surface and retained austenite of the material, are measured with GE/Seifert XRD in Metal Forming Center of Excellence at Atılım University (Figure 3.8).



Figure 3.8. Residual stress measurement with XRD.

X-ray measurements were carried out  $\sin^2 \psi$  technique and Cr-K $\alpha$  radiation on crystallographic planes of steel. Since the peak shift at high diffraction angles is significantly higher, peak having high intensity is preferred for measurements. The intensity and angular position data for analysis is ensured by scintillation detector and scalar. Parabola method was used for the determination of the maximum peak point and position of it. Then, corresponding values for interplanar spacing and strains are calculated. Finally, the stress was determined by linear regression analysis by determining the slope of the regression line of lattice strain corresponding  $\sin^2 \psi$  plot and multiplying it with elastic modulus of the material (Şimşir and Gür, 2008).

Measurement parameters were chosen in Table 3.4.

Table 3.4. Analysis parameters for XRD

Material	Iron
Radiation	Cr-K $\alpha$
Poisson's Ratio, $\nu$	0.28
Young Modulus, $E$	211,000 MPa
Diffraction Angle, $\theta$	156.1°
Lattice Planes, hkl	211

Stresses are calculated with Equation 3.1:

$$\sigma = \frac{E}{1+\nu \sin^2 \psi} \frac{d_\psi - d_0}{d_0} \quad \text{Equation 3.1}$$

In equation 3.1,  $d_0$  is spacing between planes at initial state,  $d_\psi$  is spacing between planes at  $\psi$  slope angle,  $E$  is modulus of elasticity,  $\nu$  is Poisson's ratio.

The most important advantage of XRD is capable of measurement of residual stress on surface. But residual stress measurement of depth profiles with XRD is possible with technique called electro polishing which is very long term and expensive process. As for the stress on the depth profile is measured with hole drilling method based on ESPI technique.

Residual stress measurements were done Stresstech-Prism Hole drilling equipment in Metal Forming Center of Excellence in Atılım University (Figure 3.9).

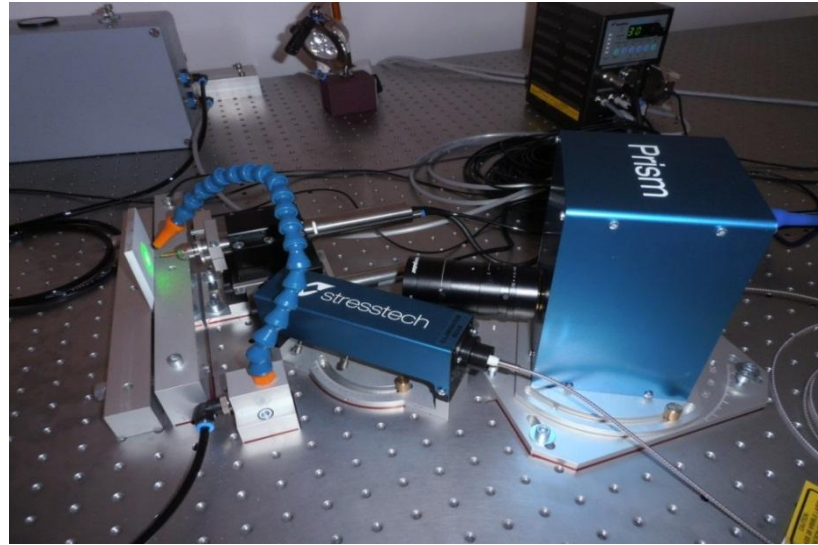


Figure 3.9. Hole drilling equipment.

ESPI system is faster than strain gages method and it is more appropriate for various material types. Furthermore, it gives detailed information about deformations appearing as a result of hole drilling. There is no need for strain gages and preparation of materials (Steinzig and Ponslet, 2003).

Tangential and axial stresses in specimens were determined in 0.5, 0.75, 0.1, 0.15, 0.2, 0.25, 0.3, 0.4, 0.5 mm depth profile shown in Figure 3.10. The drill is made by tungsten carbide coated with TiN and has a nominal diameter of 0.8 mm.

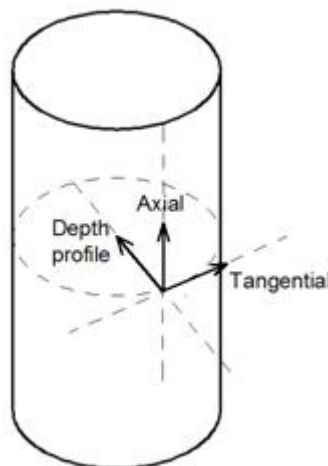


Figure 3.10 Tangential and axial components of residual stress and direction of depth profile.

### 3.3 Microstructure Examination

The microstructure analysis of the materials is significant as it paves the way to compare the effects of various heat treatments to the internal structure of the material. For microstructure analysis, specimens are prepared as follows (Figure 3.10):

- Specimens with 20 mm in diameter and 50 mm in length are cut with EDM in 10 mm heights.
- Specimens are sanded with 180-320-600-800-1000-1200  $\mu\text{m}$  sanders, respectively.
- Sanded specimens are refurbished with 3  $\mu\text{m}$  diamond paste.
- Refurbished surfaces are etched with 2% nital etching solution.

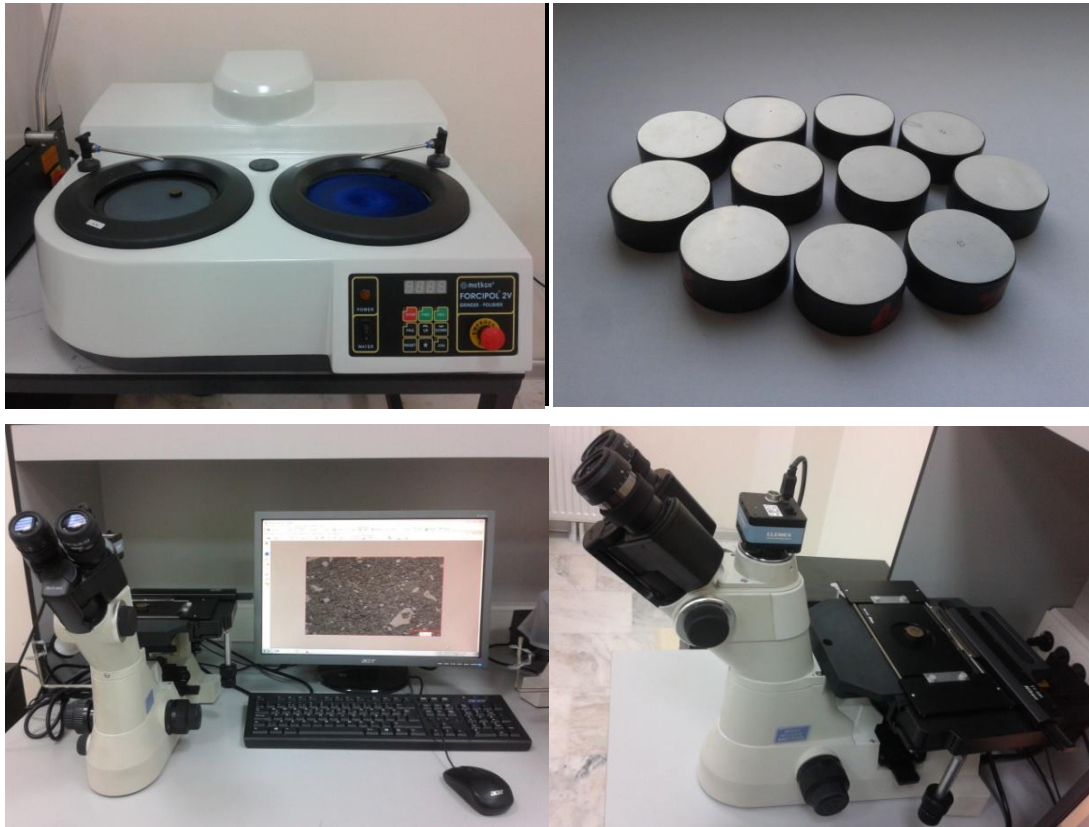


Figure 3.10. Microstructure examinations.

Specimens are cut in Metal Forming Center of Excellence in Atılım University and prepared for metallographic examination with *STRUERS DAP-7* grinding/polishing machine in Material Engineering laboratory in the Faculty of Technology of Gazi University. Microstructure images of the specimens prepared of metallographic examination, are taken with *Nikon* optical microscope in Material Engineering laboratory of Yıldırım Beyazıt University. In addition, phase analysis was carried out by means of *GE/Seifert XRD* in Metal Forming Center of Excellence in Atılım University.

### 3.4 Hardness Measurement

The researches related with effects of holding times at cryogenic temperature on hardness of die/tool steels are few in number and have contradictory results. In Table 3.5, summary of effect of sub-zero treatments on hardness in different steels is seen.

Table 3.5. Effects of sub-zero treatments on hardness of steels (Das et al., 2010).

Steel	Variation of hardness	Author
AISI T1 steel	Marginal improvement (2.0%) by DCT	Yun et al. (1998)
AISI M2 steel	Marginal improvement (2.0%) by DCT	Yun et al. (1998)
AISI D2 steel	Marginal improvement by CT, SCT and DCT	Collins and Dormer (1997)
4340 steel	Marginal improvement (2.4%–3.0%) by DCT	Zhirafar et al. (2007)
AISI D2 steel	Marginal improvement by DCT	Wierszylowski et al. (2006)
AISI D2 steel	Improvement at lower tempering temperature but reduction at higher tempering temperature by DCT	Rhyim et al. (2006)
AISI D2 steel	Marginal improvement by CT, SCT or DCT	Surberg et al. (2008)
PM S390 MC high speed steel	Marginal improvement by DCT	Cajner et al. (2009)
AISI M2 steel	Considerable improvement (8.2%) by DCT	Molinari et al. (2001)
AISI H13 steel	Negligible improvement (0.04%) by DCT	Molinari et al. (2001)
Case carburized En 353 steel	Marginal improvement (3.5%) by both CT and DCT	Prabhakaran et al. (2005)
En 31 bearing steel	Significant improvement by CT (18.8%) and by DCT (21.6%)	Harish et al. (2009)

Before the hardness of the specimens were measured, their surfaces were sanded with 180-320  $\mu\text{m}$  sanders. Thus the surface of specimens were polished and made ready for a healthy measurement. After, hardness of the specimens were measured in a lab of Yıldırım Beyazıt University. *Q-ness* macro hardness tester was used for measurement and measuring unit was determined as Rockwell C (150 kg). Values were measured in 10 different points and their arithmetic average was taken (Figure 3.11).



Figure 3.11. Macro hardness tester.

### 3.5 Grinding the Specimens and Measurement of Surface Roughness

Measurement of surface roughness with profilometry is widely used in industry and this method is repeatable, cost-efficient and easy to evaluate. Average value of surface roughness is shown with  $Ra$  ( $\mu\text{m}$ ) symbol.  $Ra$  value is value of average of rise (positive direction) and fall (negative direction) in nominal surface (Figure 3.12).

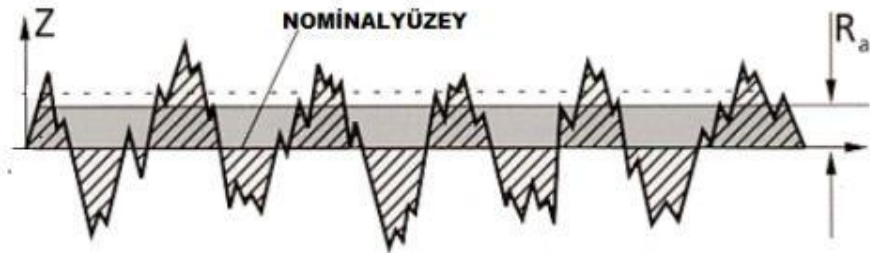


Figure 3.12. Average surface roughness value,  $Ra$ .

$Ra$  value is evaluated with Equation 3.2 (İşbilir, 2006):

$$Ra = \frac{1}{lr} \int_0^1 |Z(x)| dx \quad \text{Equation 3.2}$$

$lr$  : reference length

$Z(x)$  : deviation of the roughness curve from a mean line of the roughness curve

$x$  : profile direction

Grinding process was done in BE-TA Engine-Cover Renewal Plant. As a grinding, wheel aluminum oxide ( $Al_2O_3$ ), grain size of 60, was chosen. The diameter of the wheel was 200 mm and the thickness was 20 mm. Grinding parameters were the same for every specimen and they were grinded in 1450 revolution per minute (rpm) with 0.2 mm depth of cut. As a cooler, boron oil was used during grinding.

Surface roughness measurement was done with *SJ-201 Mitutoyo* surface roughness tester. Firstly, tester was calibrated using standard gauge. Until  $2.97 \mu\text{m}$



surface roughness of standard gauge was obtained, measurements were carried on (Figure 3.13). Measurements were taken from 4 various direction with  $0^\circ$ ,  $45^\circ$ ,  $90^\circ$  and  $135^\circ$  (Figure 3.14). Surface roughness value was determined by taking the arithmetic average of the values. The measuring length was set as  $0.8 \times 5 = 4$  mm.



Figure 3.13. Calibration of tester.



Figure 3.14. Measurement of surface roughness.



## CHAPTER 4

### RESULTS AND DISCUSSIONS

#### 4.1 Residual Stress

Residual stresses in axial direction are seen in Figure 4.1. According to graph, while stress on surface of specimen conventionally treated is 321,5 MPa, stress on surface of specimens cryotreated considering holding times at cryogenic temperature are 313 MPa for  $t_{CT} = 30$  min, 207.7 MPa for  $t_{CT} = 4$  h, 283.6 MPa for  $t_{CT} = 16$  h, and 242.3 MPa for  $t_{CT} = 24$  h. Although all surfaces have tensile residual stress, in comparison to conventional heat treatment, cryogenic treatment decreases the stresses. Reduction in stress are 35%  $t_{CT} = 4$  h, 24.6% for  $t_{CT} = 24$  h, 11.7% for  $t_{CT} = 16$  h, 2.6% for  $t_{CT} = 30$  min, respectively. Tensile residual stress turn into compressive residual stress as from depth of 0.25 mm for  $t_{CT} = 16$  h, 30 min, and 24 h. But in specimen conventionally treated and cryotreated for  $t_{CT} = 4$  h, tensile stress keeps on till 0.5 mm.

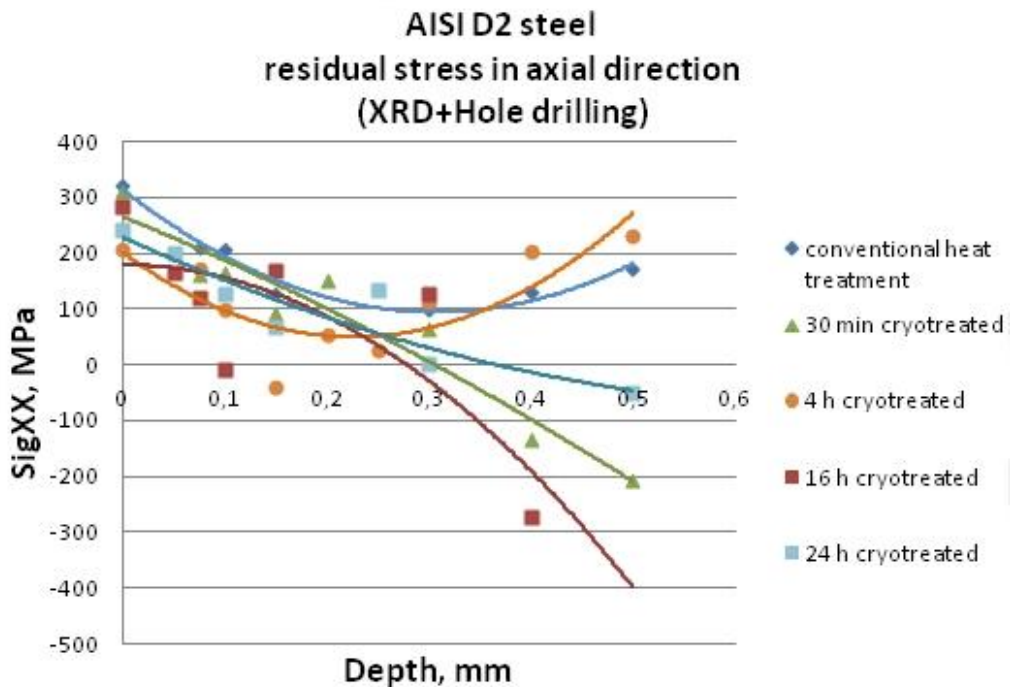


Figure 4.1. Residual stress in axial direction.

The difference of residual stress between various holding times and conventional cryogenic treatment is seen better in Figure 4.2. It is possible to say that tensile stresses on surface decrease by cryogenic treatment. Depending on holding time at cryogenic temperature, tensile stresses tend to reduction.

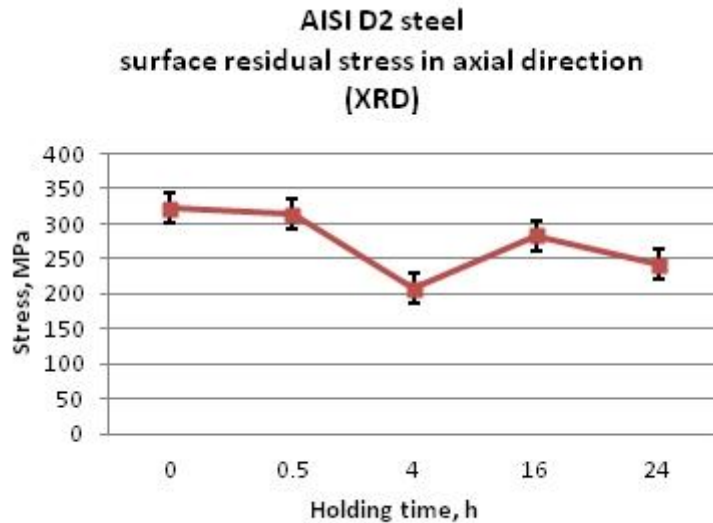


Figure 4.2 Surface residual stress in axial direction.

In tangential direction, it is obtained similar results with axial direction (Figure 4.3). As all surfaces have tensile residual stress, cryogenic process provides reduction of stress. Stress on surface of specimen conventionally treated is 316,8 MPa and stress on surface of specimens cryotreated considering holding times at cryogenic temperature are 231.4 MPa for  $t_{CT} = 30$  min, 274.1 MPa for  $t_{CT} = 4$  h, 259.6 MPa for  $t_{CT} = 16$  h, and 172.5 MPa for  $t_{CT} = 24$  h. Reduction in stress are 45.5% for  $t_{CT} = 24$  h, 26.9% for  $t_{CT} = 30$  min, 13.47% for  $t_{CT} = 4$  h, 18% for  $t_{CT} = 16$  h, respectively. Tensile residual stress turn into compressive residual stress as from depth of 0.3 mm for  $t_{CT} = 30$  min, 16 h, and 24 h. But in specimen conventionally treated and cryotreated for  $t_{CT} = 4$  h, tensile stress keeps on till 0.5 mm.

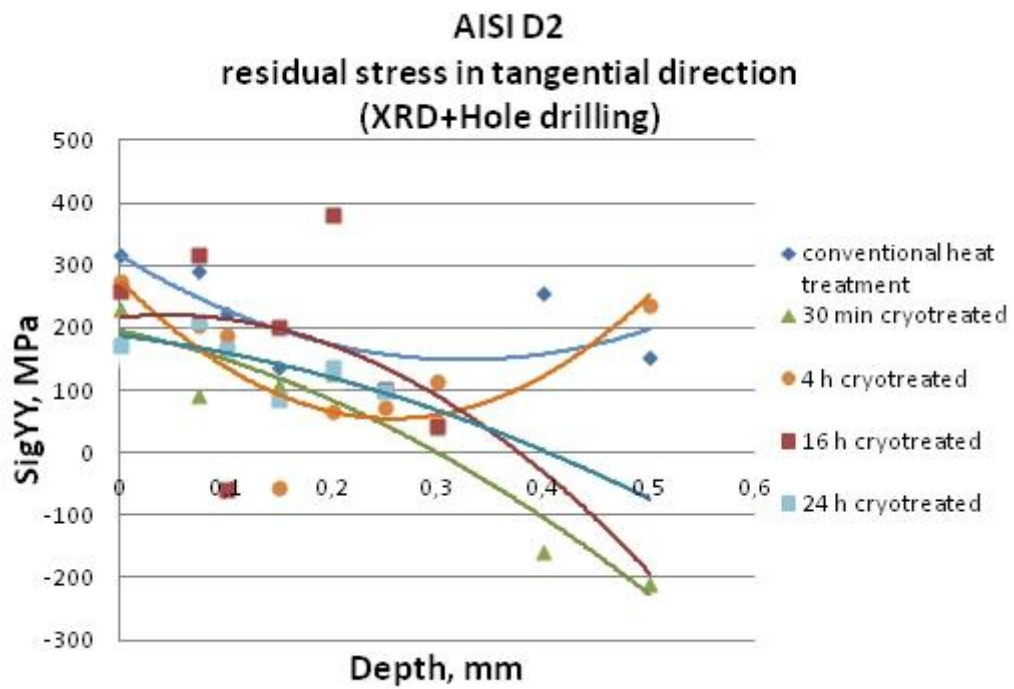


Figure 4.3. Residual stress in tangential direction.

It is seen that tensile stress decreases with cryogenic treatment and highest reduction occurs for  $t_{CT} = 24$  h (Figure 4.4).

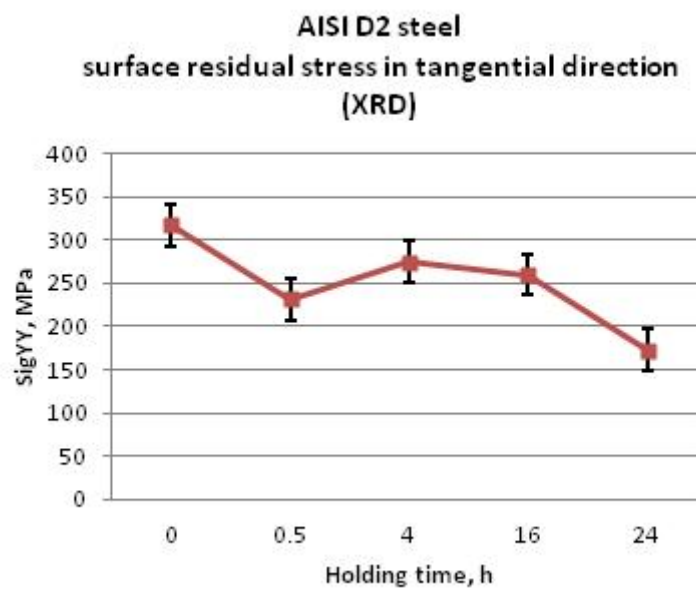


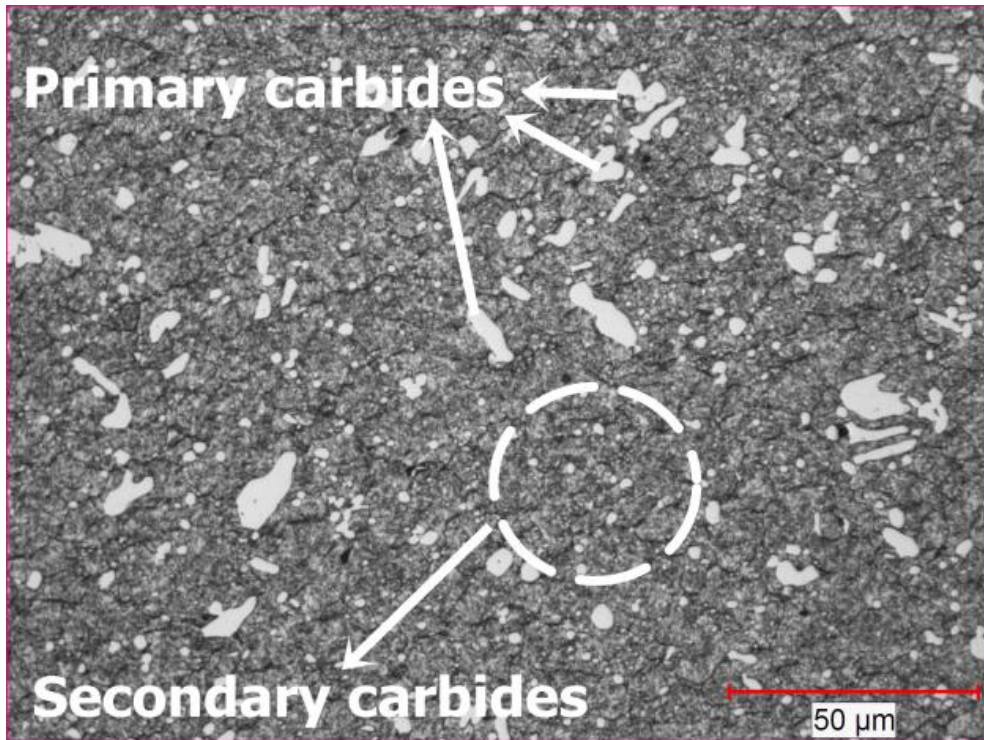
Figure 4.4 Surface residual stress in tangential direction.

## 4.2 Microstructural Characteristics

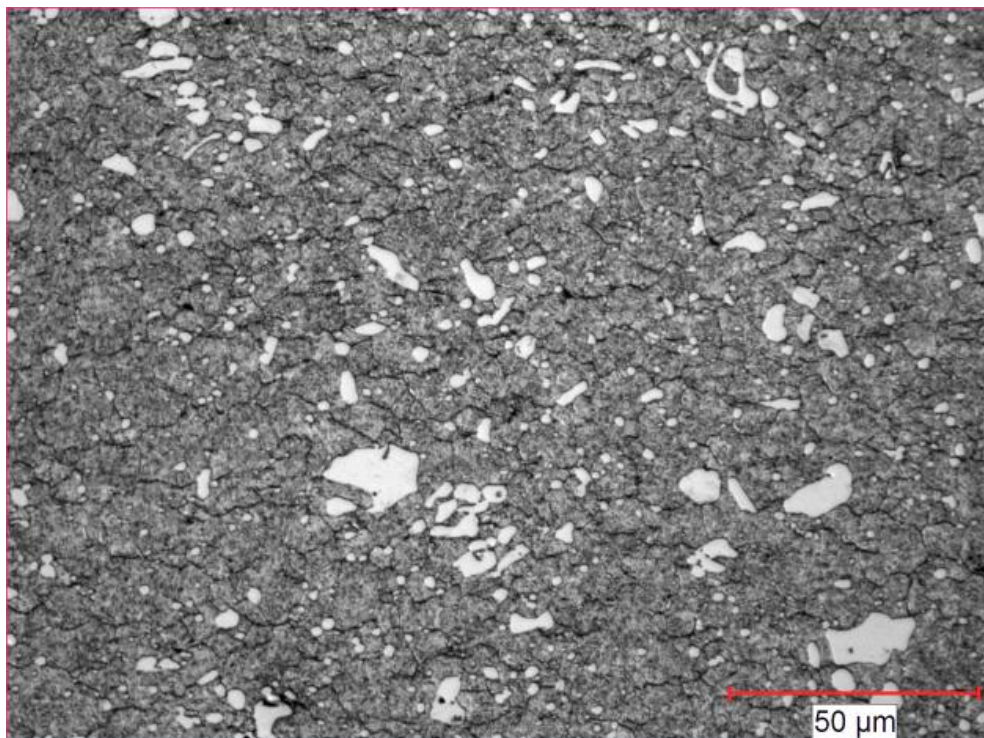
After specimens were examined with optical microscopy, for each specimen micrographs were taken in different magnification. As a result of phase analysis with XRD, carbides seen in Figure 4.5 and Figure 4.6 are chrome carbides ( $Cr_7C_3$ ). Das et al. categorize carbides as primary carbides (size > 5  $\mu\text{m}$ ) and secondary carbides (size  $\leq 5$   $\mu\text{m}$ ). It is known that cryogenic treatment increases number of secondary carbides and provides uniform distribution (Das et al., 2009a, 2009c, 2010a, 2009d, 2009e, 2010b; Das et al., 2007; Das and Ray, 2012a, 2012b; Das et al., 2009; Das et al., 2010). As shown in Figure 4.5 (a) conventional heat treatment and (e) 24 h cryogenic treatment, and Figure 4.6 (a) conventional heat treatment and (e) 24 h cryogenic treatment, areas marked indicate primary and secondary carbides. In comparison to conventional heat treatment, there is marginally variation in carbides for  $t_{CT} = 30$  min, 4 and 16 h, but for  $t_{CT} = 24$  h number of carbides increases considerably.

Collins and Dormer (1997), and Yun (1998) suggested that longer holding times at cryogenic temperature enhanced distribution of fine carbides. In another research, for  $t_{CT} = 0$  min, 1, 12, 36, 60, 84 and 132 h, it was seen that number of secondary carbides increases up to 36 h. It is possible to say that more spherical and finer secondary carbides precipitate for  $t_{CT} = 24$  h. Besides, more homogenous distribution occurs for  $t_{CT} = 24$  h.

Difference between carbides distribution of specimen conventionally treated and cryotreated can be seen better in Figure 4.5 for x500 magnification. More homogenous precipitation of secondary carbides are clearly observed in Figure 4.5 (e).

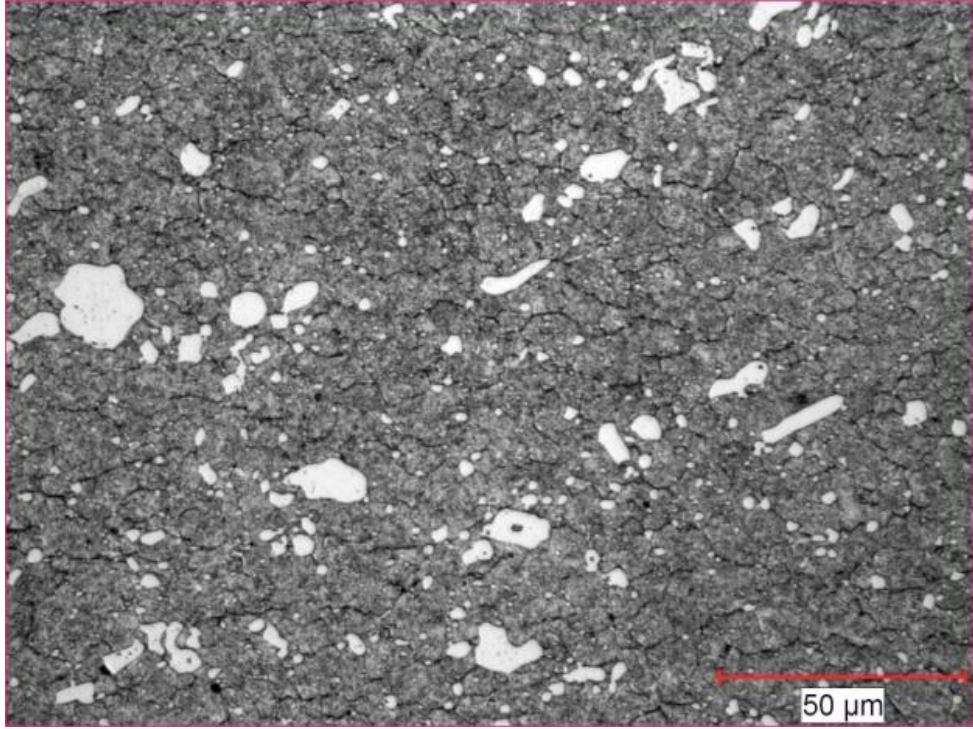


a) Specimen conventionally treated.

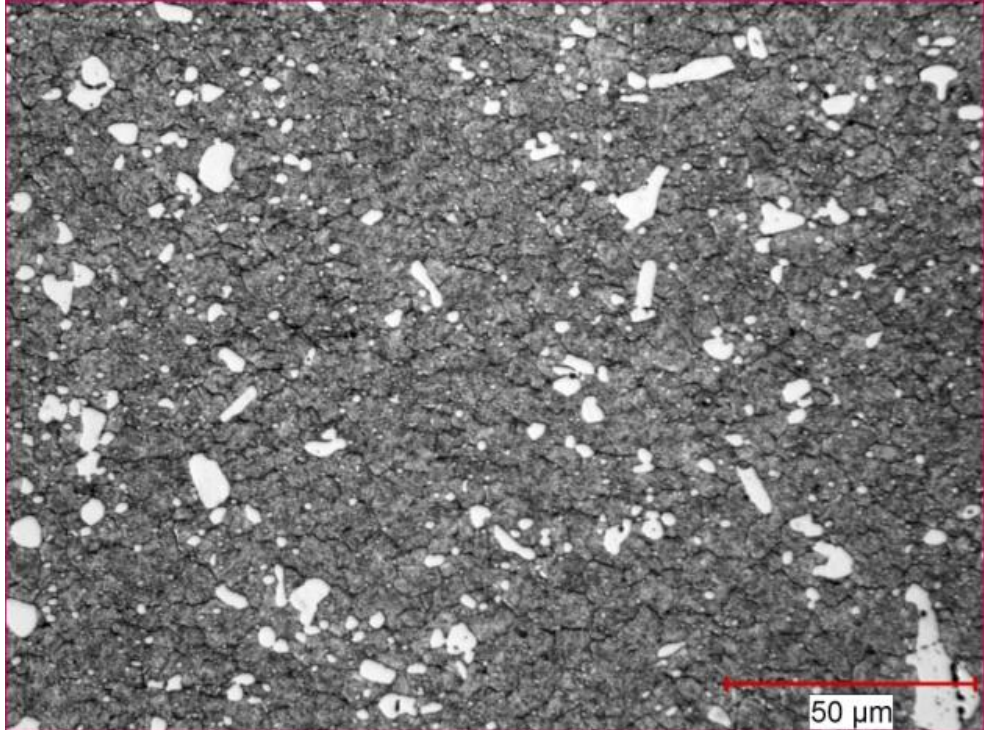


b) 30 min cryogenic treatment.

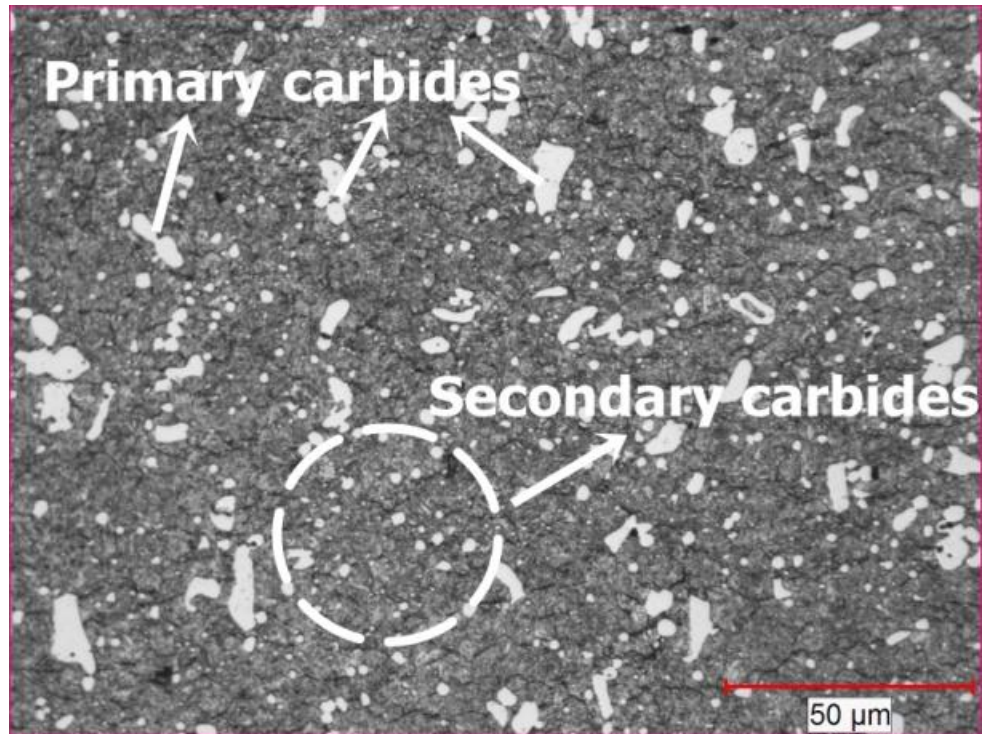




c) 4 h cryogenic treatment.

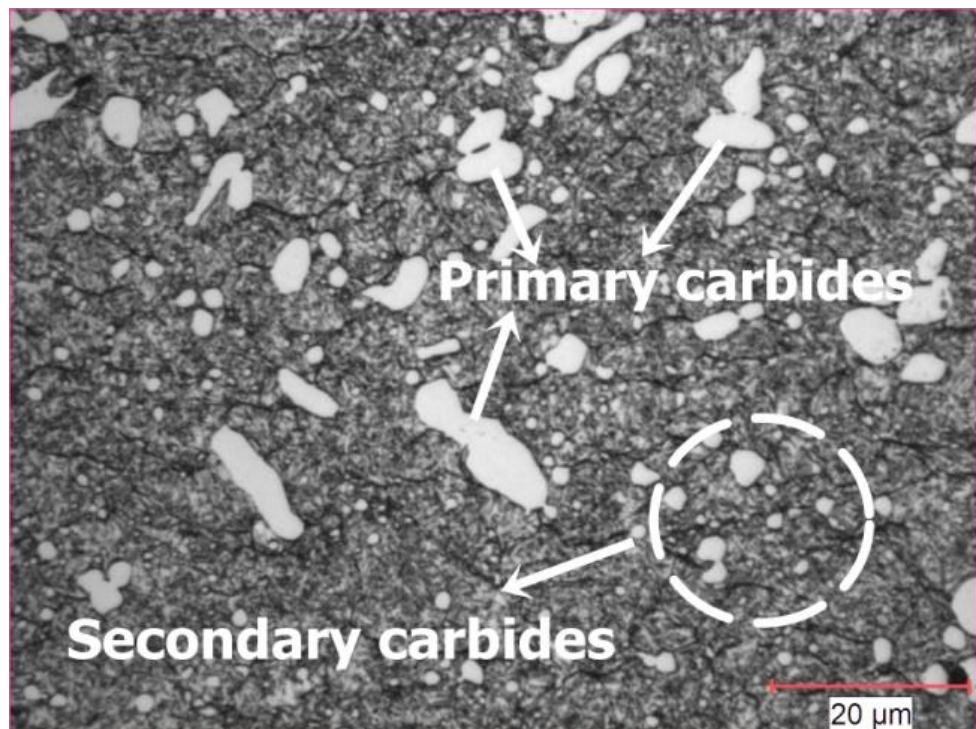


d) 16 h cryogenic treatment.



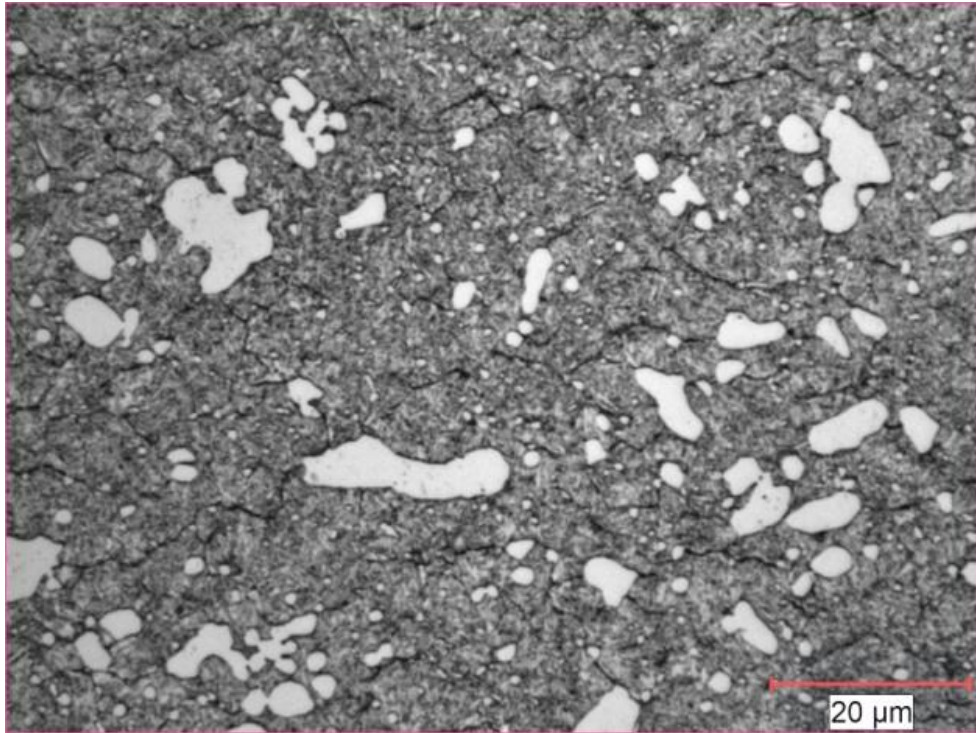
e) 24 h cryogenic treatment.

Figure 4.5. Microstructure of specimens (X500 magnification).

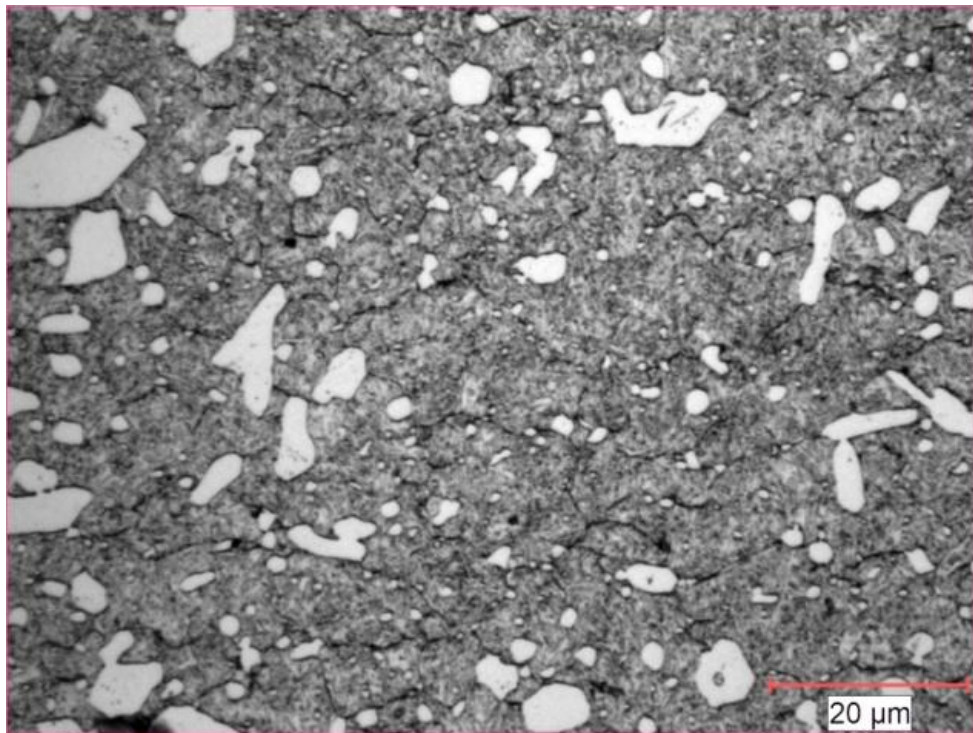


a) Specimen conventionally treated.



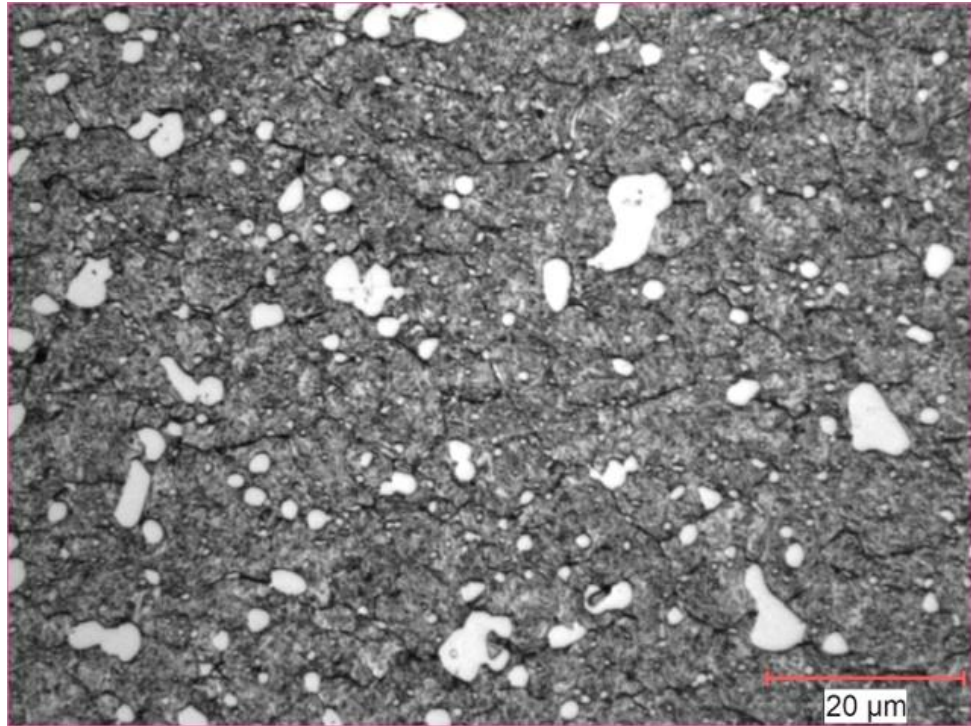


b) 30 min cryogenic treatment.

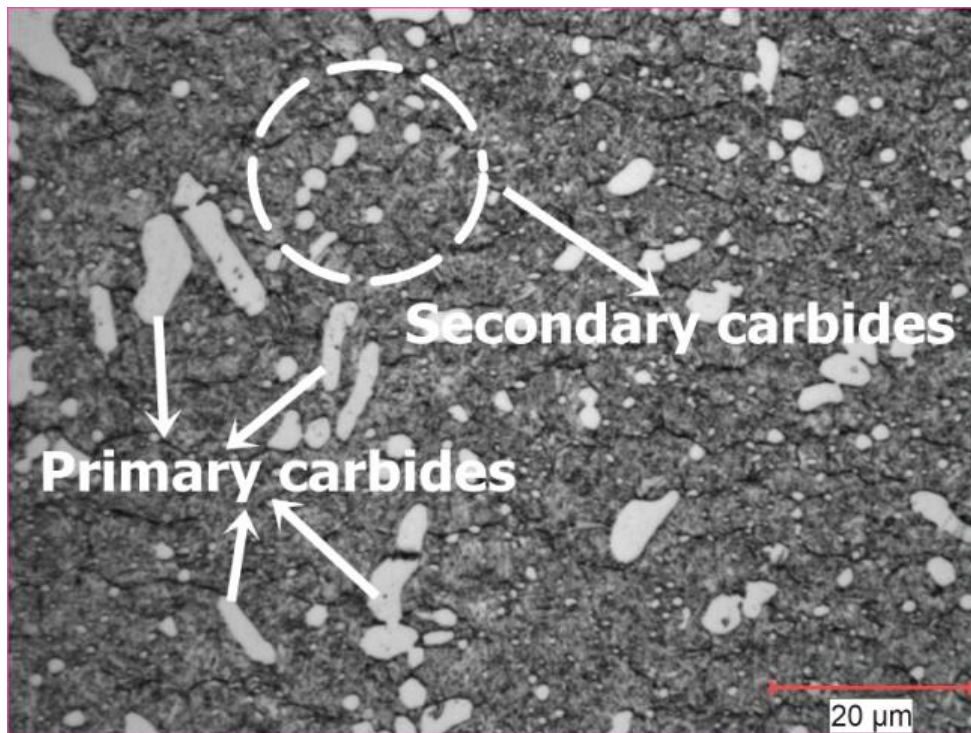


c) 4 h cryogenic treatment.





d) 16 h cryogenic treatment.



e) 24 h cryogenic treatment.

Figure 4.6. Microstructure of specimens (X1000 magnification).

### 4.3 Retained Austenite

Volume fraction of retained austenite was analysed by XRD and results are shown in Figure 4.7. The specimens conventional treated and cryotreated for  $t_{CT} = 4, 16$  and 24 h contain about 1 vol.% of retained austenite and it can be said that nearly all of retained austenite transforms to martensite phase. Only the specimen for  $t_{CT} = 30$  min contains 2 vol.% of retained austenite. But it can be considered that any significant difference between retained austenite content of specimens conventional treated and cryotreated occurs, since high tempering temperature cause transformation from austenite to martensite. Yun et al. (1998) suggested that retained austenite phase did not depend on time in contrast to carbide distribution. In Figure 4.7 shows that there is no variation in volume fraction of retained austenite by longer holding times.

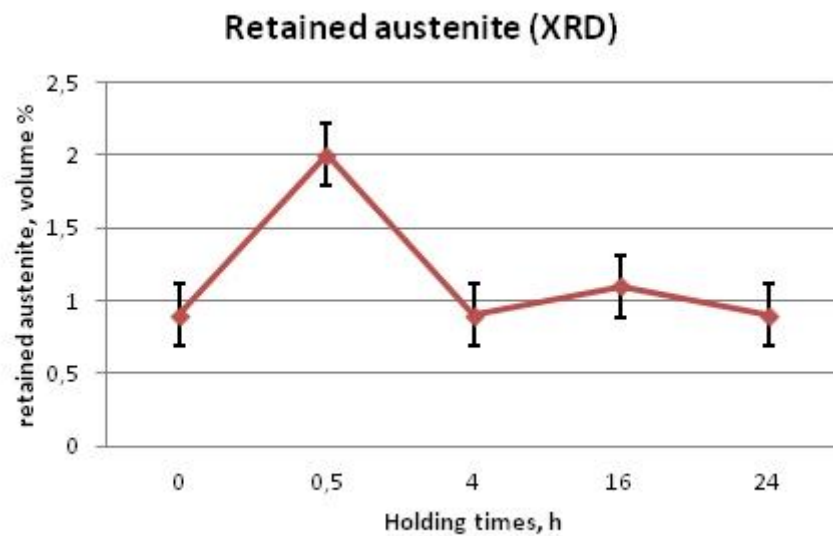


Figure.4.7 Retained austenite in AISI D2 steel.

#### 4.4 Hardness Values

Macro hardness values of specimens are shown in Figure 4.8. Results indicate that hardness of specimens cryotreated is lower than specimen conventionally treated. There is no difference between hardness of outer diameter and inner diameter.

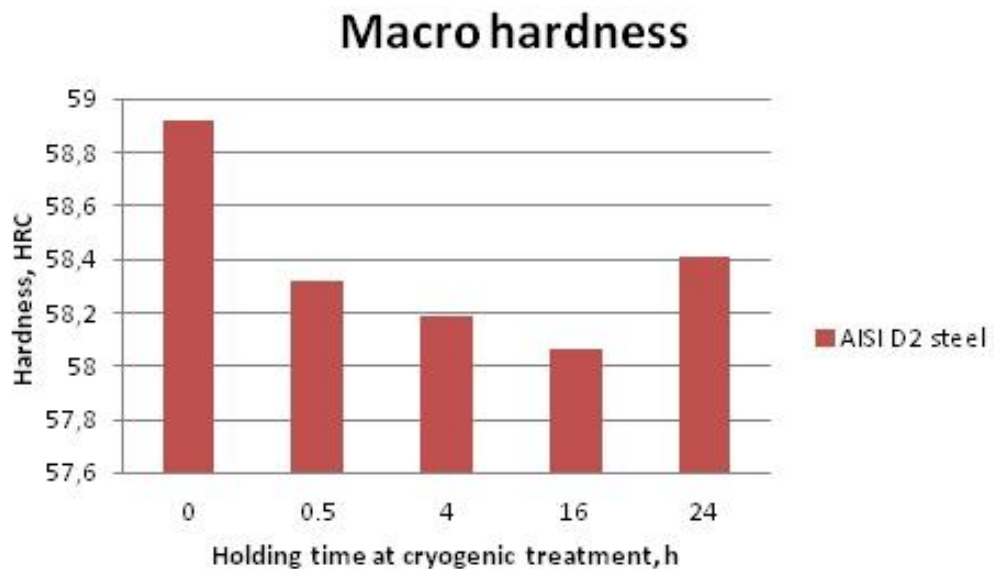


Figure 4.8. Macro hardness values of AISI D2 steel.

Hardness of the specimen conventionally treated is 58.9 HRC. Reduction of hardness occur 0.83% for  $t_{CT} = 24$  h, 0.98% for  $t_{CT} = 30$  min, 1.2% for  $t_{CT} = 4$  h, 1.42% for  $t_{CT} = 16$  h, respectively. In comparison to conventional heat treatment, minimum reduction is observed for  $t_{CT} = 24$  h. Table 3.5 shows that 2% or 3% increment in hardness are considered marginal (Zhirafar et al., 2007; Prabhakaran et al., 2005). Therefore, it can be said that hardness values have marginal decrease for various holding times.

As to reasons of reduction, Rhyim et al. (2006) suggested that tempering at low temperature improves hardness but high tempering temperatures decreases hardness. Based on this, it can be say that temperature chosen for tempering (525 °C) causes a little reduction of hardness.

#### 4.5 Surface roughness values

It can be seen that surface roughness values of AISI D2 steel in Figure 4.9. According to the graph, roughness decreases for specimens cryotreated in comparison to conventionally treated one. Reduction of roughness are 20% for  $t_{CT} = 30$  min, 12% for  $t_{CT} = 4$  h, 4.5% for  $t_{CT} = 24$  h, respectively. For  $t_{CT} = 16$  h, there is no significant difference by comparison with conventional heat treatment. Maximum reduction occurs for  $t_{CT} = 30$  min.

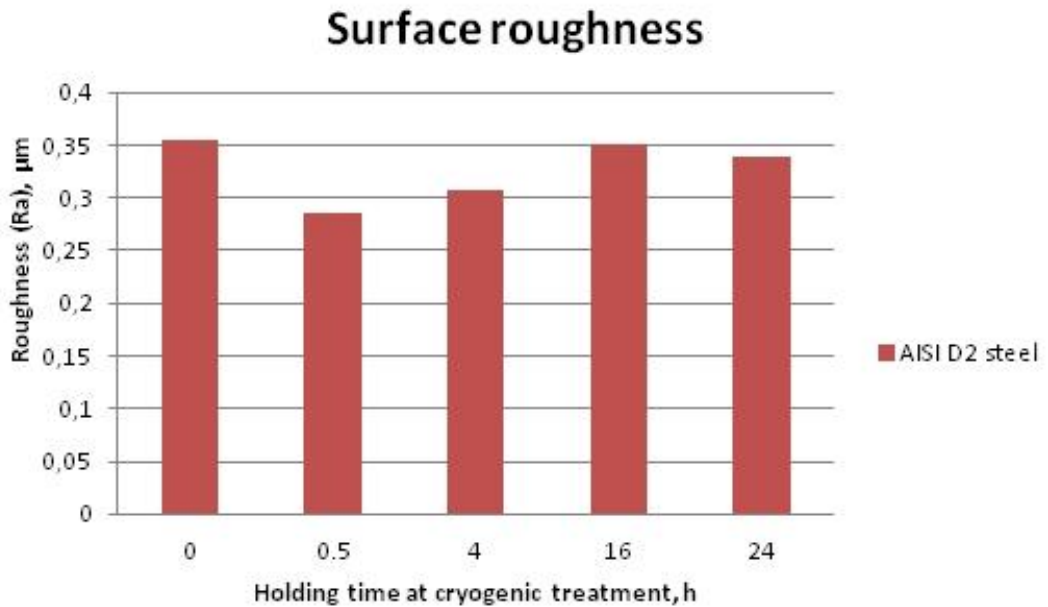


Figure 4.9. Average surface roughness (Ra) of AISI D2 steel.

#### **4.6 Correlations of Microstructure and Hardness**

In literature survey, researches related with hardness and cryogenic treatment have contradictory results. While variation in hardness is negligible in some studies (Molinari et al., 2001) and in another one says that reduction in hardness (Rhyim et al., 2006). As it is known from literature studies that retained austenite, distribution of alloying elements, and grain size are the factors effecting hardness.

When micrographs are examined, more uniform precipitation and significant increase in number of carbides comes out for  $t_{CT} = 24$  h. Whereas it has should been highest hardness value for  $t_{CT} = 24$  h, specimen conventionally treated has the highest hardness. But difference between hardness of specimen conventionally treated and cryotreated for  $t_{CT} = 24$  h is marginal according to literature, therefore it is possible to say that  $t_{CT} = 24$  h can be preferred in terms of microstructure and hardness. Cold work tool steel AISI D2 must have 54-61 HRC hardness in service conditions. In Figure 4.8, hardness of specimens cryotreated remains within this limitation.

#### **4.7 Correlations of Microstructure and Residual Stress**

Cryogenic treatment provides more uniform finer carbide precipitation and increase number of them, subsequently decrease residual stresses in material as it is mentioned Chap. 2. In Figure 4.2 and 4.3, it is seen that cryogenic treatment decrease the stresses on surfaces of AISI D2 steel. Considering holding time at cryogenic temperature, uniform and finer distribution of carbides occurs for  $t_{CT} = 24$  h which in turn residual stress diminishes most on surface of AISI D2 steel.

#### 4.8 Correlations of Microstructure, Hardness, Residual Stress and Surface Roughness

Tempering after cryogenic treatment increases carbide precipitation together with some decrease in hardness and results in reduction of residual stress in material. Reduction of residual stress and hardness leads to decrease of crack propagation and brittleness. Also, reduction in hardness provides to facilitate of machining materials which in turn surface roughness of material improves. Roughness values in Figure 4.9 show that surface of specimen conventionally treated are rougher than specimen cryotreated. Minimum roughness occurs for  $t_{CT} = 30$  min. Besides, it is seen that having more uniform carbides distribution for  $t_{CT} = 24$  h provides smoother surface. Therefore, it can be said that  $t_{CT} = 24$  h have optimum conditions regarding surface roughness, microstructure, hardness and residual stress state at the same time.

#### 4.9 Conclusions

Experimental results show:

1. Cryogenic treatment at various holding times decrease tensile stress on surface of AISI D2 steel in comparison to conventional heat treatment and convert tensile stress into compressive stress on subsurface. Due to the fact that tensile stress on subsurface accelerate the crack propagation, compressive stress on subsurface gains importance. Tensile residual stress turn into compressive residual stress as from depth of 0.3 mm for  $t_{CT} = 30$  min, 16 and 24 h.
2. Tempering at high temperature after for various holding times at cryogenic temperature does not generate significant difference in hardness. Hardness has negligible decrease in specimens cryotreated. But high tempering temperature allows some decrease in hardness by decreasing residual stress.
3. High tempering temperature cause to transformation to martensite in all specimens and any differences don not occur in volume fraction of retained austenite.

4. Microstructure of specimens for  $t_{CT} = 24$  h has more uniform carbide distribution, and number of carbides tend to increase in comparison to conventional heat treatment, but there is no considerable difference for  $t_{CT} = 30$  min, 4 and 16 h.
5. Surface roughness values of specimens cryotreated (except from  $t_{CT} = 16$  h) decreases in comparison to conventional heat treatment. Specimen conventionally treated which have highest hardness and surface residual stress represents a rough surface characteristic.
6. Results represent that  $t_{CT} = 24$  h provides lower residual stress and surface roughness and uniform and a number of carbide distribution. In this investigation optimum holding time at cryogenic temperature is 24 h regarding surface roughness, microstructure, retained austenite, hardness and residual stress state at the same time.

#### 4.10 Recommendations

Several recommendations for the future researches are listed as below.

1. The effects of longer holding times at cryogenic temperature on residual stress could be examined for AISI D2 steel or other tool/die steel.
2. Residual stress of AISI D2 steel could be investigated for various austenization and tempering temperatures or multiple tempering cycle.
3. Micrographs of carbides could be obtained for higher magnification by Scanning Electron Microscope (SEM).
4. The volume percents, size, population density and interparticle spacing of primary and secondary carbides could be estimated by image analyses of digitally acquired suitable optical.
5. Wear resistance and fatigue life of AISI D2 tool steel cryotreated could be examined.

## REFERENCES

Akhbarizadeh, A., Golozar, M.A., Shafyei, A., & Kholghy, M., Effects of austenizing time on wear behavior of D6 tool steel after deep cryogenic treatment, *J Iron Steel Res*, 16, 29-32, 2009.

Asi, O., & Can, A.Ç., Sementasyon çeliklerinde körsertleştirilmiş ve sementasyon yapılmış durumlarda meydana gelen artık gerilmelerin karşılaştırılması, *Mühendislik Bilimleri Dergisi*, 7 (2), 2001, 183-187.

Baldissera, P., & Delprete, C., Deep cryogenic treatment, a bibliographic review, *Open Mechanical Engineering Journal*, 2 (1), 2008; 1–11.

Barron, R.F., Cryogenic treatment of metals to improve wear resistance, *Cryogenics*, 22 (5), 1982, 409-413.

Bensely, A., Prabhakaran, A., Mohan Lal, D., & Nagarajan, G., Enhancing the wear resistance of case carburized steel (En 353) by cryogenic treatment, *Cryogenics*, 45 (12), 2005, 747-754.

Bensely, A., Venkatesh, S., Mohan Lal, D., Nagarajan, G., Rajadurai, A., & Junik, K., Effect of cryogenic treatment on distribution of residual stress in case carburized En 353 steel, *Materials Science and Engineering*, 479 (1-2), 2008, 229–235.

Bowes, R.G., *Heat Treat. Met.*, vol. 1, 1974, 29-32.

Carlson, E.A., *Heat Treating*, (10th ed.), ASM International, Metals Park, Ohio, 1990, 203–206.

Cajner, F., Leskovšek, V., Landek, D., Cajner, H., *Mater. Manuf. Process* 24, 2009, 743–746.



Cheng, L., Brakman, C.M., Korevaar, B.M., & Mittemeijer, E.J., The tempering of iron-carbon martensite; dilatometric and calorimetric analysis, *Metall. Mater. Trans.*, A19, 1988, 2415-2426.

Cheng, L., van der Pers, N.M., Böttger, A., de Keijser, Th.H., & Mittemeijer, E.J., Lattice changes of iron-carbon martensite on aging at room temperature, *Met. Trans. A.*, 22A, 1991, 1957-1967.

Choudhury, S.K., & Bajpai, J.B., Investigation in orthogonal turnmilling towards better surface finish, *Journal of Materials Processing Technology*, 170, 2005, 487-493.

Collins, D.N., & Dormer, J., Deep cryogenic treatment of a D2 cold-work tool steel, *Heat Treatment Met.*, 3, 1997, 71-74.

Collins, D. N., Deep cryogenic treatment of tool steels: a review, *Heat Treatment of Metals*, 23 (2), 1996, 40–42.

Das, D., Ph.D. Thesis, Bengal Engineering and Science University, Shibpur, Howrah, India, 2011.

Das, D., Dutta, A. K., Toppo, V., & Ray, K.K., Effect of deep cryogenic treatment on the carbide precipitation and tribological behavior of D2 steel, *Materials and Manufacturing Processes*, 22, 2007, 474-480.

Das, D., Dutta, A. K., & Ray, K. K., On the enhancement of wear resistance of tool steels by cryogenic treatment, *Philosophical Magazine Letters*, 88, 2008, 801-811.

Das, D., Dutta, A. K., & Ray, K. K., On the refinement of carbide precipitates by cryotreatment in AISI D2 steel, *Philosophical Magazine*, 89, 2009a, 55-76.

Das, D., Dutta, A. K., & Ray, K. K., Inconsistent wear behaviour of cryotreated tool steels: role of mode and mechanism, *Materials Science and Technology*, 25, 2009b, 1249-1257.

Das, D., Dutta, A. K., & Ray, K. K., Influence of varied cryotreatment on the wear behavior of AISI D2 steel. *Wear*, 266, 2009c, 297-309.

Das, D., Dutta, A. K., & Ray, K. K., Correlation of microstructure with wear behaviour of deep cryogenically treated AISI D2 steel, *Wear*, 267, 2009d, 1371-1380.

Das, D., Dutta, A. K., & Ray, K. K., Optimization of the duration of cryogenic processing to maximize wear resistance of AISI D2 steel, *Cryogenics*, 49, 2009e, 176–184.

Das, D., Ray, K.K., & Dutta, A.K., Influence of temperature of sub-zero treatments on the wear behaviour of die steel, *Wear*, 267, 2009, 1361-1370.

Das, D., Dutta, A. K., & Ray, K. K., Sub-zero treatments of AISI D2 steel: Part I. Microstructure and hardness. *Materials Science and Engineering*, 527, 2010a, 2182–2193.

Das, D., Dutta, A. K., & Ray, K. K., Sub-zero treatments of AISI D2 steel: Part II. Wear behavior, *Materials Science and Engineering*, 527, 2010b, 2194–2206.

Das, D., Sarkar R., Dutta, A. K., & Ray, K. K., Influence of sub-zero treatments on fracture toughness of AISI D2 steel, *Materials Science and Engineering*, 528, 2010, 589-603.

Das, D., & Ray, K. K., Structure–property correlation of sub-zero treated AISI D2 steel, *Materials Science and Engineering*, Volume, 541, 2012a, 45-60.

Das, D., & Ray, K. K., On the mechanism of wear resistance enhancement of tool steels by deep cryogenic treatment, *Philosophical Magazine Letters*, 92 (6), 2012b, 295-303.

Determining Residual Stresses by the Hole Drilling Strain Gage Method, ASTM Standard Test Method E837-99, American Society for Testing and Materials, 1999.

Dülek, E., Ç 1020 Malzemedeki Bilyalı Dövme ile Oluşturulan Yüzeydeki Kalıcı Gerilmelerin Katman Kaldırma (Elektro Kimyasal) Yöntemiyle İncelenmesi, Master Thesis, Gazi University, Institute of Science and Technology, 2002.

Ekmekci B., Theoretical and Experimental Investigation of Residual Stresses in Electric Discharge Machining, Ph.D. Thesis, The Middle East Technical University, 2004.

Farhani, F., Niaki, K. S., Vahdat, S. E., & Firozi, A., Study of effects of deep cryotreatment on mechanical properties of 1.2542 tool steel, *Materials and Design*, 42, 2012, 279–288.

Fukaura, K., Yokoyama, Y., Yokoi, D., Tsujii, N., & Ono, K., Fatigue of cold-work tool steels: effect of heat treatment and carbide morphology on fatigue crack formation, life, and fracture surface observations, *Metallurgical And Materials Transactions A*, 35A, 2004.

Gauthier, M.M., *Engineered Materials Handbook*, (Desk Edition), ASM International, Materials Park, OH, U.S.A., 1995.

Guu, Y.H., & Hocheng, H., Improvement of fatigue life of electrical discharge machined AISI D2 tool steel by TiN coating. *Materials Science and Engineering*, 318, 2001, 155–162.

Guu, Y.H., Hocheng, H., Chou, C.Y., & Deng, C.S., Effect of electrical discharge machining on surface characteristics and machining damage of AISI D2 tool steel, *Materials Science and Engineering A*, 358, 2003, 37-43.

Harish, S., Bensely, A., Mohan Lal, D., Rajadurai, A., Gyongyver, B., & Lenkey, J., Microstructural study of cryogenically treated En 31 bearing steel, *Journal of Materials Processing Technology*, 209, 2009, 3351–3357.

Hanabusa, T., Scholtes, B., & Macherauch, E., X-ray residual stress measurement of a plus b brass after uniaxial tensile deformation, In: 29th Japan congress on materials research, Tokyo, 1985, 123–6.

Handbook of Measurement of Residual Stresses, Society for Experimental Mechanics, Edited by Lu, J., US, 1996.

Huang, J.-H., Ouyang, F.-Y., & Yu, G.-P., Effect of film thickness and Ti interlayer on the structure and properties of nanocrystalline TiN thin films on AISI D2 steel, *Surface & Coatings Technology*, 201, 2007, 7043–7053.

Huang, J.Y., Zhu, Y.T., Liao, X.Z., Beyerlein, I.J., Bourke, M.A., & Mitchell, T.E., Microstructure of cryogenic treated M2 tool steel, *Materials Science and Engineering*, A339, 2003, 241–244.

Imamura, S., Fukui, H., Shibata, A., Omori, N., & Setoyama, M., Properties and cutting performance of AlTiCrN/TiSiCN bilayer coatings deposited by cathodic-arc ion plating. *Surface & Coatings Technology*, 202, 2007, 820–825.

Kafkas, F., Katman Kaldırma Teknigine Dayalı Olarak Kalıcı Gerilmelerin Ölçülmesini Sağlayan Bilgisayarlı Ölçme Cihazının Tasarımı ve İmalatı, Master Thesis, Gazi University, Institute of Science and Technology, 2001.

Kamody, D., Process for the cryogenic treatment of metal containing materials", US Patent 5, 259, 1993, 200.

Macherauch E., Introduction to residual stress, Advances in surface treatments: 4, Residual stresses, Pergamon Oxford, 1987,1-35.

Meng, F., Tagashira, K., Azuma, R., & Sohma, H., Role of etacarbide precipitations in the wear resistance improvements of Fe-12Cr-Mo-V-1.4C tool steel by cryogenic treatment, ISIJ International, 34, 1994, 205–210.

Mohan Lal, D., Renganarayanan, S., & Kalanidhi A., Cryogenic treatment to augment wear resistance of tool and die steels, Cryogenics, 41, 2001, 149-155.

Molinari, A., Pellizzari, M., Gialanella, S., Straffelini, G., & Stiasny, K.H., Effect of deep cryogenic treatment on the mechanical properties of tool steels, Journal of Materials Processing Technology, 118, 2001, 350-355.

Moore, K.E., & Collins, D.N., Cryogenic treatment of three heat-treated tool steels, Key Engineering Materials, 86–87, 1993, 47–54.

Nomak Akdoğan, A., Kalıp yüzeylerinin ve proses sırasındaki değişimlerinin geometrik mamul şartları temelinde incelenmesi ve modellenmesi, Ph.D. Thesis, Yıldız Technical University, Institute of Science and Technology, 2005.

Oppenkowski, A., Weber, S., & Theisen, W., Evaluation of factors influencing deep cryogenic treatment that affect the properties of tool steels. Journal of Materials Processing Technology, 210, 2010, 1949-1955.

Özay, Ç., Ballıkaya, H., & Savaş, V., 304 östenitik paslanmaz çeliğinin teğetsel tornalama-frezeleme yöntemi ile işlenmesinde yüzey pürüzlülüğünün araştırılması, 6th International Advanced Technologies Symposium (IATS'11) Elazığ, 2011.

Pan, W.L., Yu, G.P., & Huang, J.H., Mechanical properties of ion-plated TiN films on AISI D2 steel, *Surface Coating Technology*, 110, 1998, 111-119.

Rossini, N.S., Dassisti, M., Benyounis, K.Y., & Olabi, A.G., Methods of measuring residual stresses in components, *Materials and Design*, 35, 2012, 572–588.

Popandopulo, A.N., & Zhukova, L.T., Transformations in high-speed steels during cold treatment. *Metal Science and Heat Treatment*, 22, 1980, 708–710.

Rankin, J.E., Hill, M.R., & Hackel L.A., The effects of process variations on residual stress in laser peened 7049 T73 aluminum alloy, *Volume*, 43 (1), 2003, 97-104.

Rhyim Y.M., Han S.H., Na Y.S., & Lee J.H., Effect of deep cold cryogenic treatment on carbide precipitation and mechanical properties of tool steels, *Solid State Phenomena*, 118, 2006, 9-14.

Roberts, G., Krauss, G., & Kennedy, R., *Tool Steels*, (5th ed.), ASM International, Materials Park, OH, 1998.

Sarga, P., & Menda, F., Comparison of Ring-Core Method and Hole-drilling Method Used for Determining Residual Stresses, *American Journal of Mechanical Engineering*, 1 (7), 2013, 335-338.

Stresstech Oy., *Residual Stress Measurement by Prism*, 2013.

Paulin, P., Frozen Gears, *Gear Technology*, 10, 1993, 26-29.

Prabhakaran, A., Bensely, A., Nagarajan, G., & Mohan Lal, D., *Proc. Int. Mech. Eng. Conf.*, 2004, 1–5.

Reed-Hill R.E., & Abbaschian, R., *Physical Metallurgy Principles*, (3rd Ed.), PWS-Kent Publishing Company, Boston, MA, 1992.

Roberts, G., Krauss, G., & Kennedy, R., Tool Steels, (5th ed.), ASM International, Metals Park, OH, 1998.

Schajer, G.S., Residual Stresses: Measurement by Destructive Testing, Encyclopedia of Materials: Science and Technology, 2001, 8152–8158.

Schajer, G.S., H-Drill, Hole Drilling Residual Stress Calculation Program User Guide, Canada, 2001, 1-46.

Scott, H., Scientific Papers, Bureau of Standards, 16, 1920, 521–536.

Sen, S., Ozbek, I., Sen, U., & Bindal, C., Mechanical behavior of borides formed on borided cold work tool steel, Surface Coating Technology, 135, 2001, 173-177.

Senthilkumar, D., Rajendran, I., Pellizzari, M., & Siiriainen, J., Influence of shallow and deep cryogenic treatment on the residual state of stress of 4140 steel, Journal of Materials Processing Technology, 211, 2011, 396–401.

Şimşir, C., & Gür, H., 3D FEM simulation of steel quenching and investigation of the effect of asymmetric geometry on residual stress distribution of materials, Journal of Material Processing Technology, 207, 2008, 211–221.

Skalli, N., & Flavenot, J.F., Prise en compte des contraintes résiduelles dans un calcul prévisionnel de tenue en fatigue, CETIM-Information, 90, 1985, 35-47.

Sohar, C.R., Betzwar-Kotas, A., Gierl, C., Weiss, B., & Danninger, H., Gigacycle fatigue behavior of a high chromium alloyed cold work tool steel. International Journal of Fatigue, 30, 2008, 1137–1149.

Steinzig, M., & Ponslet, E., Residual stress measurement using the hole drilling method and laser speckle interferometry: Part 1, 27 (3), 2003, 43-46.

Surberg, C.H., Stratton, P., & Lingenh le, K., The effect of some heat treatment parameters on the dimensional stability of AISI D2, *Cryogenics*, 48, 2008, 42–47.

Takım elikleri El Kitabı, Assab & Korkmaz.

Taylor, K.A., Olson, G.B., Cohen, M., & Vander Sande, J.B., Carbide precipitation during stage I tempering of Fe-Ni-C martensites, *Metallurgical Transactions A*, 20, 1989, 2749–2765.

Tebedge, N., Alpsten, G., & Tall, L., Residual-stress measurement by the sectioning Method, *Experimental Mechanics*, 13 (2), 1973, 88–96.

Thelning, K.E., *Steel and Its Heat Treatment* (2nd ed.), Butterworths, London, 1984.

Thornton, R., Slatter, T., Jones, A.H., & Lewis, R., The effects of cryogenic processing on the wear resistance of grey cast iron brake discs, *Wear*, 271, 2011, 2386– 2395.

Tiziani, A. Molinari, Improvement of AISI D2 steel properties by unconventional vacuum heat treatments, *Materials Science and Engineering: A*, 10, 1988, 125–133.

Totten, G., Howes, M., & Inoue, T., *Hand-book of Residual Stress and Deformation of Steel*, ASM International, Materials Park, OH, 2002.

Unterweiser, P.M., Boyer, H.E., Kubbs, J.J., *Hear Treater’s Guide—Standard Practices and Procedures for Steel*, (4th ed.), ASM International, Metal Park, Ohio, 1987, 300–312.

Varol, R. & Bedir, F., Artık Gerilmelerin  nemi ve Yorulma Limiti  zerine Etkisi, *M hendis ve Makine*, 34 (406), 1993, 38-41.

Wierszylowski, I., *Defect Diff. Forum*, 258–260, 2006, 415–420.



Withers, P.J., & Badeshia, H.K.D.H., Residual Stress, Part 1- Measurement Techniques, *Materials Science and Technology*, 17, 2001, 355-365.

Yelbay, H.İ., Tahribatsız Yöntemlerle Kalıntı Gerilim Ölçümündeki Gelişmeler, 3rd International Non-Destructive Testing Symposium and Exhibition, April 2008 Istanbul.

Yıldız, Y., & Nalbant, M., A review of cryogenic cooling in machining processes, *International Journal of Machine Tools & Manufacture*, 48, 2008, 947–964.

Yiğit, O., Dilmeç, M., & Halkacı, S., Tabaka kaldırma yöntemi ile kalıntı gerilmelerin ölçülmesi ve diğer yöntemlerle karşılaştırılması, *Mühendislik ve Makine*, 49, 2008, 20-27.

Yun, D., Xiaoping, L., & Hongshen, X., Deep cryogenic treatment of high-speed steel and its mechanism, *Heat Treatment of Metal*, 3, 1998, 55–59.

Zhang, Y., Pratihari, S., Fitzpatrick, M.E., & Edwards L., Residual Stress Mapping in Welds Using the Contour Method, *Materials Science Forum*, 490-491, 2005, 294-299.

Zhang, K.M., Zou, J.X., Bolle, B., & Grosdidier T., Evolution of residual stress states in surface layers of an AISI D2 steel treated by low energy high current pulsed electron beam, *Vacuum*, 87, 2013, 60-68.

Zhirafar, S., Rezaeian, A., & Pugh, M., Effect of cryogenic treatment on the mechanical properties of 4340 steel, *Journal of Materials Processing Technology*, 186, 2007, 298–303.

## **APPENDIX**

## Appendix 2.1. Analysis formulas of hole drilling method

$$\varepsilon_1 = A(\sigma_x + \sigma_y) + B(\sigma_x - \sigma_y)\cos 2\beta$$

$$\varepsilon_2 = A(\sigma_x + \sigma_y) + B(\sigma_x - \sigma_y)\cos 2(\beta + 45)$$

$$\varepsilon_2 = A(\sigma_x + \sigma_y) + B(\sigma_x - \sigma_y)\cos 2(\beta + 90)$$

$$\sigma_{max} = \frac{\varepsilon_1 + \varepsilon_3}{4A} - \frac{1}{4B} \sqrt{(\varepsilon_3 - \varepsilon_1)^2 + (\varepsilon_3 + \varepsilon_1 - 2\varepsilon_2)^2}$$

$$\sigma_{max} = \frac{\varepsilon_1 + \varepsilon_3}{4A} + \frac{1}{4B} \sqrt{(\varepsilon_3 - \varepsilon_1)^2 + (\varepsilon_3 + \varepsilon_1 - 2\varepsilon_2)^2}$$

$$\tan 2\beta = \frac{\varepsilon_1 - 2\varepsilon_2 + \varepsilon_3}{\varepsilon_3 - \varepsilon_1}$$

$$A = -a \frac{(1 + \nu)}{2E}$$

$$A = \frac{-a}{2E}$$